THE METEOROLOGICAL MAGAZINE

HER MAJESTY'S STATIONERY OFFICE

November 1986

Met.O.971 No. 1372 Vol. 115

THE METEOROLOGICAL MAGAZINE

No. 1372, November 1986, Vol. 115

551.509.33:551.509.5

Experimental monthly long-range forecasts for the United Kingdom

Part II. A real-time long-range forecast by an ensemble of numerical integrations

By J.M. Murphy and T.N. Palmer*

(Meteorological Office, Bracknell)

Summary

The use of an ensemble of integrations for long-range prediction has been studied with a hemispheric version of the Meteorological Office 5-level general circulation model. Some results, showing the potential of the technique, are described. The method is now being used with the global 11-level model to produce real-time long-range forecasts for the long-range forecasting conference in the Synoptic Climatology Branch of the Meteorological Office. Results from the first of these real-time ensemble forecasts are discussed.

1. Introduction

The short-range predictive skill of numerical weather prediction (NWP) models has steadily improved over the years. Despite this, attempts to use such models to forecast the instantaneous state of the atmosphere a month into the future have not enjoyed much success. The fundamental reasons for this lie not only with deficiencies in the numerical models, but also with the very equations of motion which the models integrate.

Specifically, the difference between two or more integrations of an NWP model whose initial states differ by a small amount (representing, say, analysis error) will increase with time until at some stage the integrations are completely independent of one another, in the sense that they can be thought of as random states in some climatological distribution. This suggests that the atmosphere has some 'limit of deterministic predictability' and attempts to estimate this (e.g. Lorenz 1982, Mansfield 1986) suggest that, on average, it is considerably less than 1 month. This limit can be extended by considering the model's forecast of only the planetary-scale modes and/or time-averaged fields (Shukla 1981), though this approach ignores a fundamental problem that forecasting on the monthly time-scale has a marked probabilistic element, and is not strictly deterministic. The multivariate statistical model (Maryon and Storey 1985, Folland and Woodcock 1986), the backbone of the operational long-range forecasting system in the Meteorological Office, has this notion built into its basic formulation; it does not predict one pattern of surface pressure, but assigns probabilities to a number of pre-defined patterns.

* Now on secondment to the European Centre for Medium Range Weather Forecasts, Shinfield Park, Reading.

One way of approaching the probabilistic nature of long-range forecasting using dynamical models is through the method of 'ensemble' forecasting, where the model is integrated, not from one initial state, but from a set of equally possible initial states, consistent, say, with known analysis errors. A priori each forecast from this ensemble of initial states is treated as equally likely. If, after a month of integration, each member of the ensemble has totally diverged from each of the others then no useful information can be obtained from the forecasts. If, however, subsets of the ensemble forecast tend to 'cluster together', then probabilities can be assigned to each cluster and a probabilistic forecast given.

Over the past 2 years the ensemble forecast method has been developed in the Synoptic Climatology Branch of the Meteorological Office (Mansfield 1986, Murphy 1985). This work, based on the Meteorological Office 5-level model (Corby *et al.* 1977), has shown that under certain circumstances useful information can be obtained from the ensemble technique, even out to 1 month. Some of this work is summarized in section 2. Encouraged by this research, it was decided to attempt to use the ensemble forecast technique in real time for the regular long-range forecasting conferences.

The first of these attempts took place at the mid-September 1985 conference. To the best of the authors' knowledge this was the first occasion that an ensemble of integrations of an NWP model has had a direct impact on the production of a real-time long-range forecast. The following is an account of the method used to produce this forecast, the forecast itself, and an assessment of its skill.

2. Potential impact of ensemble forecasting

Before attempting a practical real-time ensemble forecast, it was necessary to establish whether, in principle, this technique could be used to give an improvement in long-range forecast skill. If the notion of a probability distribution of forecasts, each arising from initial conditions compatible with a given initial analysis, is valid, then the mean of a finite ensemble of such forecasts should, on average, be closer to the true atmospheric evolution than should an individual forecast from within the ensemble.

To test this idea, eight 50-day ensemble forecasts, each containing seven individual integrations, were made from winter initial conditions using, in this case, the 5-level model. The ensembles were created by adding spatially correlated random perturbations to a given observed state to simulate the effects of analysis error. The method used was to take a linear combination of the observed state with an independent analysis such that the difference between the resulting perturbed state and the observed state corresponded to a typical root-mean-square (r.m.s.) analysis error of 30 metres at 500 mb. Each ensemble forecast was verified both against observations and against an additional 'nature' integration, also produced using the above perturbation technique. The purpose of the latter was to test the ensemble method under the (unrealistic) assumption that the model has no systematic biases. With this so-called 'perfect-model' assumption, the additional integration can be thought of as a possible realization of the real atmosphere and used to verify the forecasts (see Fig. 1). The predictability limit under a perfect-model assumption can be thought to provide an upper bound to the model's actual predictive skill.

Fig. 2 shows results averaged over the eight ensembles under this perfect-model assumption. All the curves refer to results for the 500 mb geopotential height field in the area 30–85° N. The skill score is defined by the 'anomaly correlation coefficient'. To calculate this, model fields are calculated relative to an estimate of the model climatology obtained by averaging over the eight 'nature' runs.

As discussed above, it is expected that, on average, the ensemble-mean forecast would yield an improvement in predictability relative to an individual forecast. However, as mentioned in the introduction, some improvement in skill may also be gained by removing the least predictable scales of motion by spatial or temporal filtering.

The curves in Fig. 2 show the relative effects of spatial filtering and ensemble averaging on forecast skill. An improvement in skill is obtained if only the long-wave component, represented by zonal waves

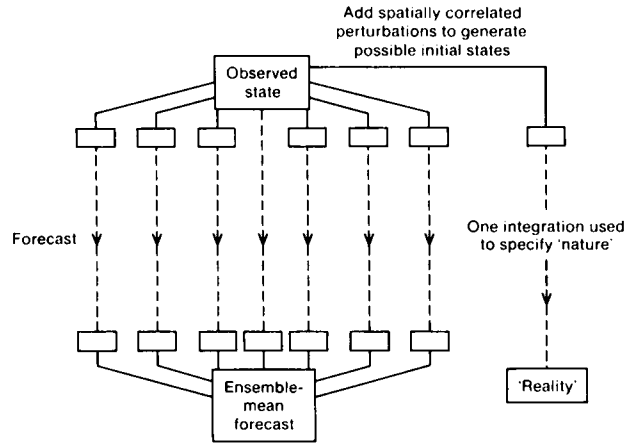

Figure 1. Schematic diagram showing the construction of a 5-level model ensemble forecast, together with the 'nature' integration used for the perfect-model evaluation of predictability.

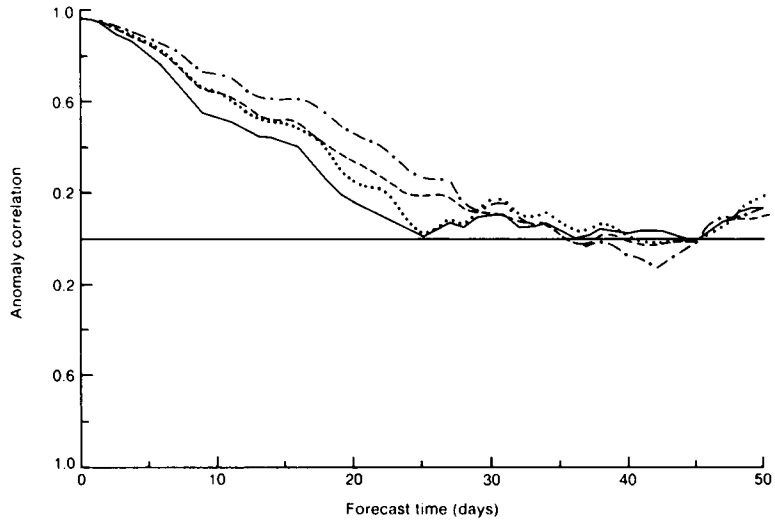

Figure 2. Average perfect-model forecast skill for 500 mb geopotential height, 30–85° N, for 5-level model integrations: ——— daily unfiltered individual forecast, ····· daily individual forecast, zonal waves 0–3 only, – – – – daily ensemble-mean forecast, —·—·— daily ensemble-mean forecast, zonal waves 0–3 only.

0–3, in an individual forecast is considered. However, if the long-wave component of the ensemble-mean forecast, formed by averaging the seven individual forecasts in a given experiment, is considered, the skill is improved still further. In terms of the predictability limit, the spatially filtered ensemble-mean forecast offers an improvement of almost 50% when compared with the unfiltered individual forecast —19 days for an individual forecast and 28 days for the spatially filtered ensemble-mean forecast.

A substantial improvement in skill can also be observed in the time-averaged ensemble-mean forecast when compared with the time-averaged individual forecast (Murphy 1985). When verified against real data, however, the ensemble-mean forecast is, on average, no better than an individual forecast. This essentially indicates that, in general, the rate of divergence of the real atmospheric evolution from the

ensemble-mean forecast is much larger than the rate of divergence of individual model forecasts from the ensemble mean.

However, even though the effect of ensemble averaging on forecast skill is negligible on average, an improvement is obtained in cases when individual forecasts show greater than average skill. In particular, in two of the eight cases, the individual forecasts were found to show skill well beyond the model's average limit of predictability (Mansfield 1986). In these two cases the ensemble-mean forecast showed a substantial improvement in skill. To investigate this further, another three random perturbation ensemble forecasts were produced for three independent situations where an individual forecast, run previously, had shown an unusually high degree of skill. In two of these three cases, the average skill of individual forecasts within the ensemble remained positive throughout, and the ensemble-mean forecast again showed a significant increase in skill. Fig. 3 illustrates the average improvement in skill given by the ensemble-mean forecast in these four unusually predictable cases compared with the effect in the other seven cases where the model did not show any skill beyond the normal predictability limit.

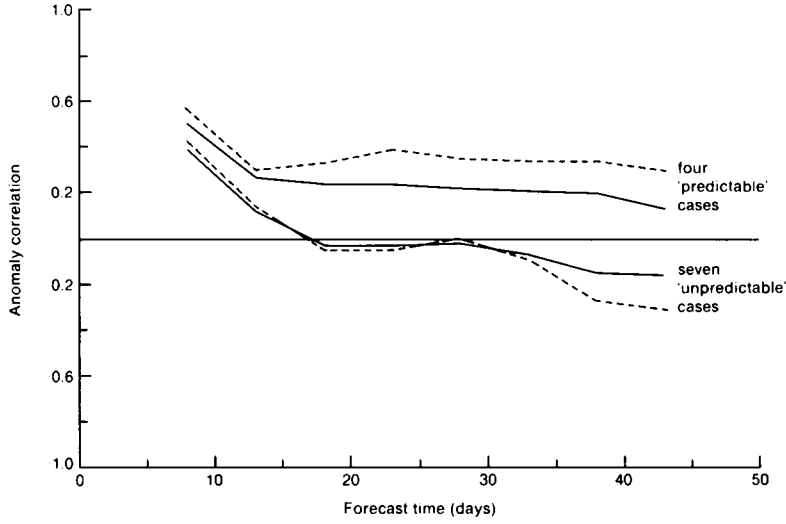

Figure 3. Practical forecast skill for four 'predictable' 5-level model forecasts and seven 'unpredictable' forecasts for the 500 mb geopotential height, 30–85° N: ——— 15-day mean individual forecast, – – – – 15-day mean ensemble-mean forecast.

3. Methodology for the real-time forecast

Having shown that increased predictability could be obtained by ensemble averaging a number of individual forecasts under perfect-model conditions, the next step was to see if a similar improvement could be obtained in reality by attempting a practical long-range ensemble forecast using a more skilful model.

The model used for the real-time integrations was the global 11-level climate model developed in the Dynamical Climatology Branch and is described in detail by Slingo (1985). The model, similar in many respects to the 5-level model, has a regular latitude–longitude grid with $2\frac{1}{2} \times 3\frac{3}{4}°$ resolution. The 11-level model was designed for long-period integrations and has an energy-conserving finite difference scheme as well as sophisticated physical parametrizations. For these reasons, it was decided that this model was the most appropriate available for long-range forecast integrations. Whilst it was not designed primarily as an NWP model, *de facto*, it is treated as such in this paper.

Instead of the spatially correlated random perturbation technique used to generate the 5-level model ensembles, seven consecutive operational analyses at 12-hour intervals between 00 GMT on 12 September 1985 and 00 GMT on 15 September 1985 inclusive were used for initial conditions for the real-time forecast. The correspondence between this 'time-lagged' technique for generating initial conditions for an ensemble and the random perturbation method depends on the forecast skill of the model, and it is still an open question as to which technique is more appropriate in practice.

The initialization dates were chosen to be as close as practicably possible to the date of the long-range forecasting conference on 17 September. As in section 2, results are expressed as anomalies with respect to an estimate of the model's autumn climatology. The latter was formed from a set of eight integrations employing a selection of initial conditions at least 10 days apart from September and October of 1983 and 1984. These integrations used climatological sea surface temperatures (SSTs).

For the forecast integrations, fixed SST anomalies, based on operational SST analyses averaged over the 10 days preceding the initialization date of the first of the forecasts, were added to an SST climatology, which was updated every 5 days during the integrations. From each forecast, time-mean fields were produced corresponding to the 5-day period immediately following the long-range forecasting conference (18–22 September), the next 10-day period (23 September–2 October), and the following 15-day period (3–17 October). (Clearly these fixed verification periods correspond to different model forecast times in each of the seven integrations.)

Results from the ensemble of forecasts (see next section) were considered, together with the multivariate statistical model, in the production of the mid-September long-range forecast.

4. Discussion of forecast

The 5 days 18–22 September represent a medium-range period of the forecast, during which there was a small spread between the ensemble members and there was a reasonable degree of skill in their predictions. Fig. 4 shows the ensemble-mean 500 mb geopotential height anomaly for this period compared with the verifying actual anomaly. Most of the major centres have a counterpart in the

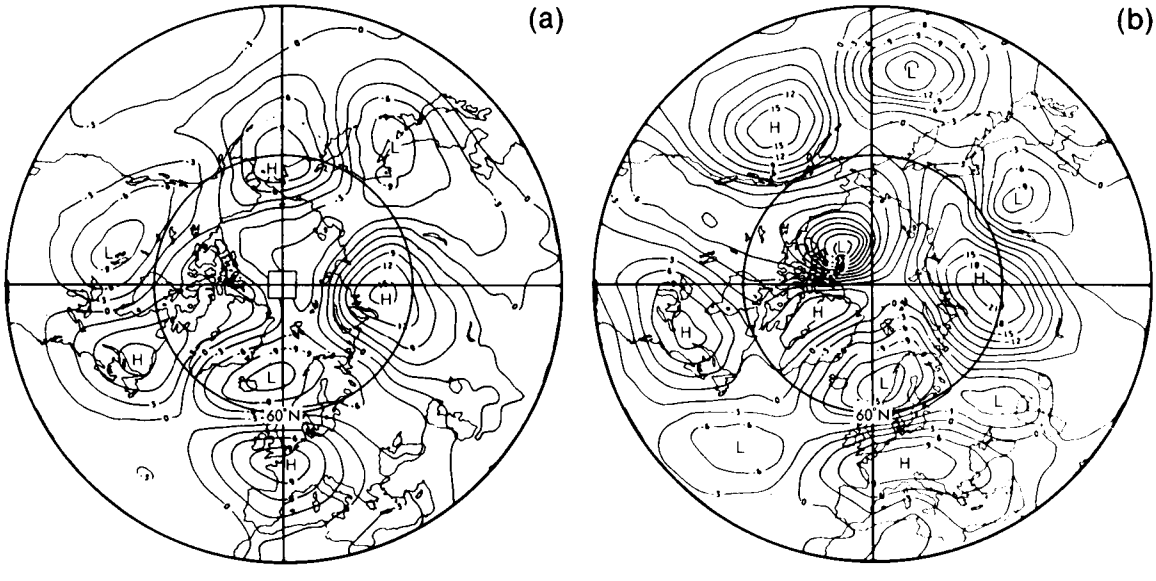

Figure 4. Ensemble-mean forecast (a) and observed (b) 500 mb geopotential height anomaly (dam) for 18–22 September 1985.

ensemble mean, the most notable exception being the deep low of −30 decametres centred near the pole. There is a fairly close correspondence between the individual forecasts in most areas at this stage (not shown); for example, all seven integrations show evidence of the high–low anomaly dipole over western Europe, a feature which corresponds well with the observed pattern in this region.

The correlation between the ensemble-mean and observed anomaly patterns, for the northern hemisphere north of 15° N, is 0.49 (Table I) — a slightly disappointing score in view of the above remarks. At this range the skill could of course be improved somewhat by weighting the more recent individual integrations more highly when forming the ensemble mean, as they are likely, on average, to be more skilful than the earlier ones (Table I confirms this in the present case). However, since the main interest is in the long-range forecast periods, for which the integrations can essentially be treated as equally likely realizations, such a procedure was not used.

The ensemble-mean forecast for the 10-day period 23 September–2 October and the actual anomaly are shown in Fig. 5. The considerable reduction in the intensity of the ensemble-mean anomaly compared with that shown in Fig. 4(a) reflects the spreading of the ensemble towards complete loss of predictability. Nevertheless, a degree of coherence still appears to exist between the individual patterns (not shown). To determine objectively whether the ensemble-mean anomaly represented anything more than random noise would require a series of point-by-point statistical Student's *t*-tests on the ensemble-mean anomaly to ascertain whether the number of points at which the anomaly was significant was greater than that expected by chance (Murphy 1985).

Table I reveals that all the individual forecasts retain a positive anomaly correlation at this stage,

Table I. *Anomaly correlations for forecast 500 mb geopotential height anomaly fields, 15–90° N for the three periods of the long-range forecast*

Integration	Forecast period		
	18–22 Sept.	23 Sept.–2 Oct.	3–17 Oct.
1 (00 GMT 12 Sept.)	0.09	0.16	−0.01
2 (12 GMT 12 Sept.)	0.21	0.10	0.08
3 (00 GMT 13 Sept.)	0.14	0.01	0.05
4 (12 GMT 13 Sept.)	0.46	0.18	−0.05
5 (00 GMT 14 Sept.)	0.51	0.34	0.09
6 (12 GMT 14 Sept.)	0.65	0.21	0.02
7 (00 GMT 15 Sept.)	0.60	0.23	−0.07
1–7 average individual forecast	0.38	0.18	0.00
1–7 ensemble-mean forecast	0.49	0.25	−0.12

although the level of correlation is low with an average score of 0.18 compared with 0.25 for the ensemble mean. This difference in skill, although modest, illustrates the principle of increasing the signal-to-noise ratio through ensemble averaging. Subjectively, most of the skill appears to lie in the eastern hemisphere, with successive centres between Europe and Kamchatka, eastern Russia corresponding quite well in position, if not intensity, with observed features. This impression is

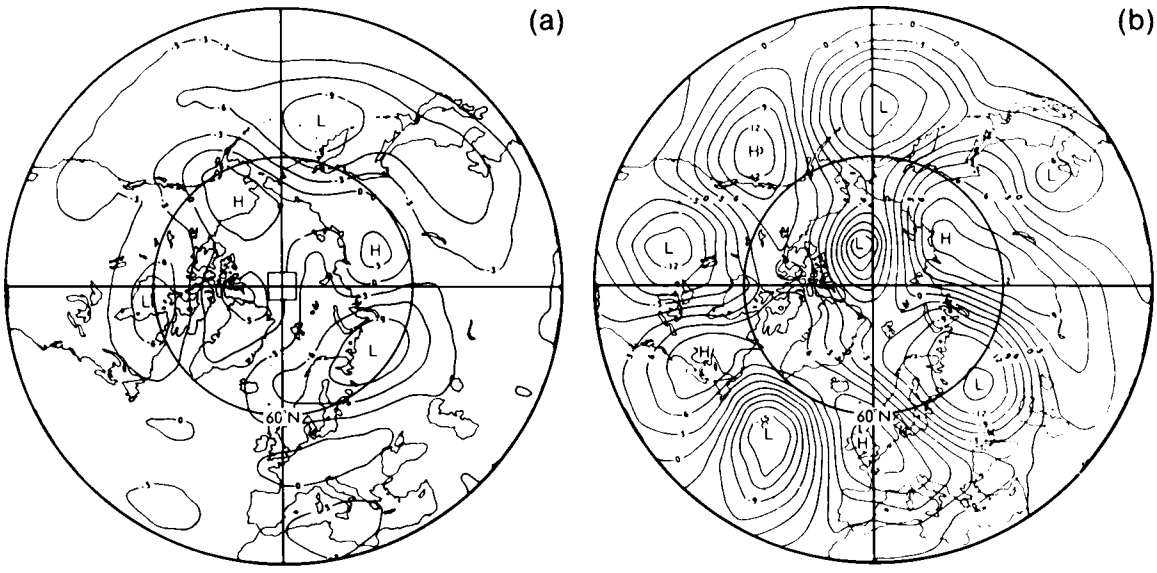

Figure 5. Ensemble-mean forecast (a) and observed (b) 500 mb geopotential height anomaly (dam) for 23 September–2 October 1985.

corroborated by limited-area anomaly correlations obtained by splitting the area north of 30° N into three equal sectors. The score for the sector 180–60° W is −0.11, whereas the scores for the sectors 60° W–60° E and 60° E–180° W are 0.39 and 0.42 respectively. Fig. 6 shows the forecasts from each integration for the 15-day period 3–17 October together with the ensemble mean. The ensemble-mean pattern has a featureless 'washed-out' nature suggesting initially that the ensemble distribution has become essentially random by this point. It is certainly true that, as measured by anomaly correlation, the forecast has completely lost skill at this stage (Table I).

The impression of the time variation of the forecast skill is obscured somewhat by using different time-averaging lengths for the three forecast periods. Accordingly, in Table II, the individual and ensemble-mean anomaly correlations obtained by splitting the forecast span into successive 5-day periods have been recorded. In terms of model time a small degree of skill remains up to days 16–20, though one cannot infer too much about the model's long-range skill from just one case. Predictability is liable to vary considerably from one experiment to another (Mansfield 1986), and also from season to season (Bengtsson and Simmons 1983).

In section 2 only the full ensemble mean of all seven integrations was considered. If an ensemble forecast is always normally distributed about its mean this is an appropriate quantity to consider. However, if, as postulated in the introduction, ensemble distributions tend to cluster into a small number of distinct groups, the full ensemble mean may become less meaningful and, alternatively, 'sub-ensemble means' should be formed from the members of each separate cluster, presenting the final forecast as a series of probabilities based on each of the sub-ensemble means.

Interestingly, there does appear to be some evidence of such clustering among the individual integrations in Fig. 6. In integrations 5–7 there is a pattern showing areas of low anomaly centred in the Pacific and near Hudson Bay with an area of high anomaly in between, somewhat similar to the winter-time Pacific/North American (PNA) pattern of Wallace and Gutzler (1981). In contrast, integrations 1–4 show no sign of this pattern, but all show a low anomaly centred near Alaska. Thus it

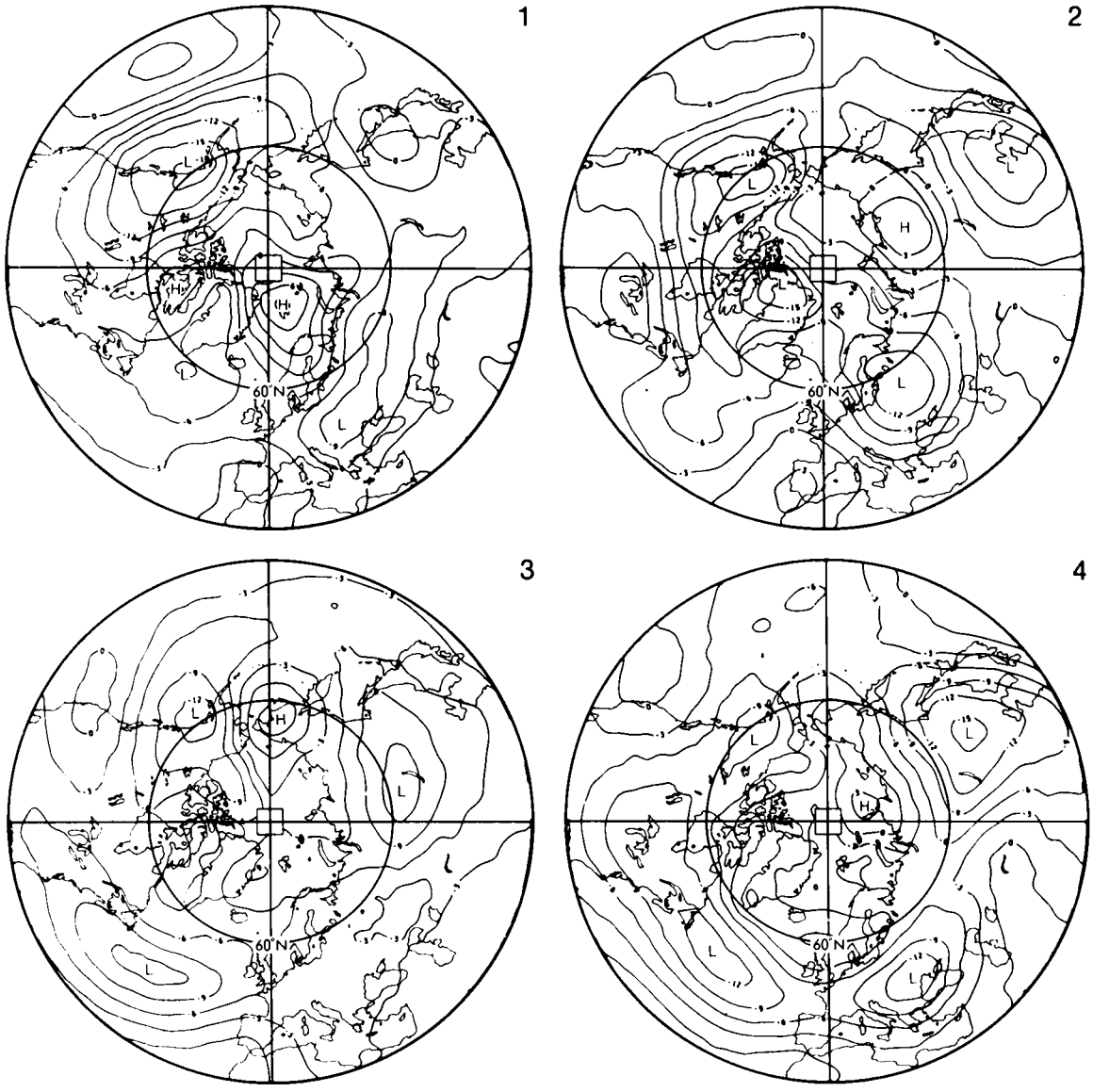

Figure 6. Individual (from integrations 1–4) forecast 500 mb geopotential height anomaly (dam) for 3–17 October 1985.

could be considered that, at least in the Pacific/North American region, the integrations have split into two definite groups. The two relevant sub-ensemble means are shown in Figs 7(a) and (b). Despite the slack pattern of the full ensemble mean this clustering suggests that the ensemble distribution has not yet become randomly distributed. Furthermore, the actual atmospheric anomaly pattern (Fig. 7(c)) in the Pacific/North American area does show a structure similar to that of the 5–7 sub-ensemble mean. However, since the latter incorrectly predicts high anomalies in polar regions and also underestimates the broadness of the high part of the pattern at lower latitudes, the correspondence in type does not show

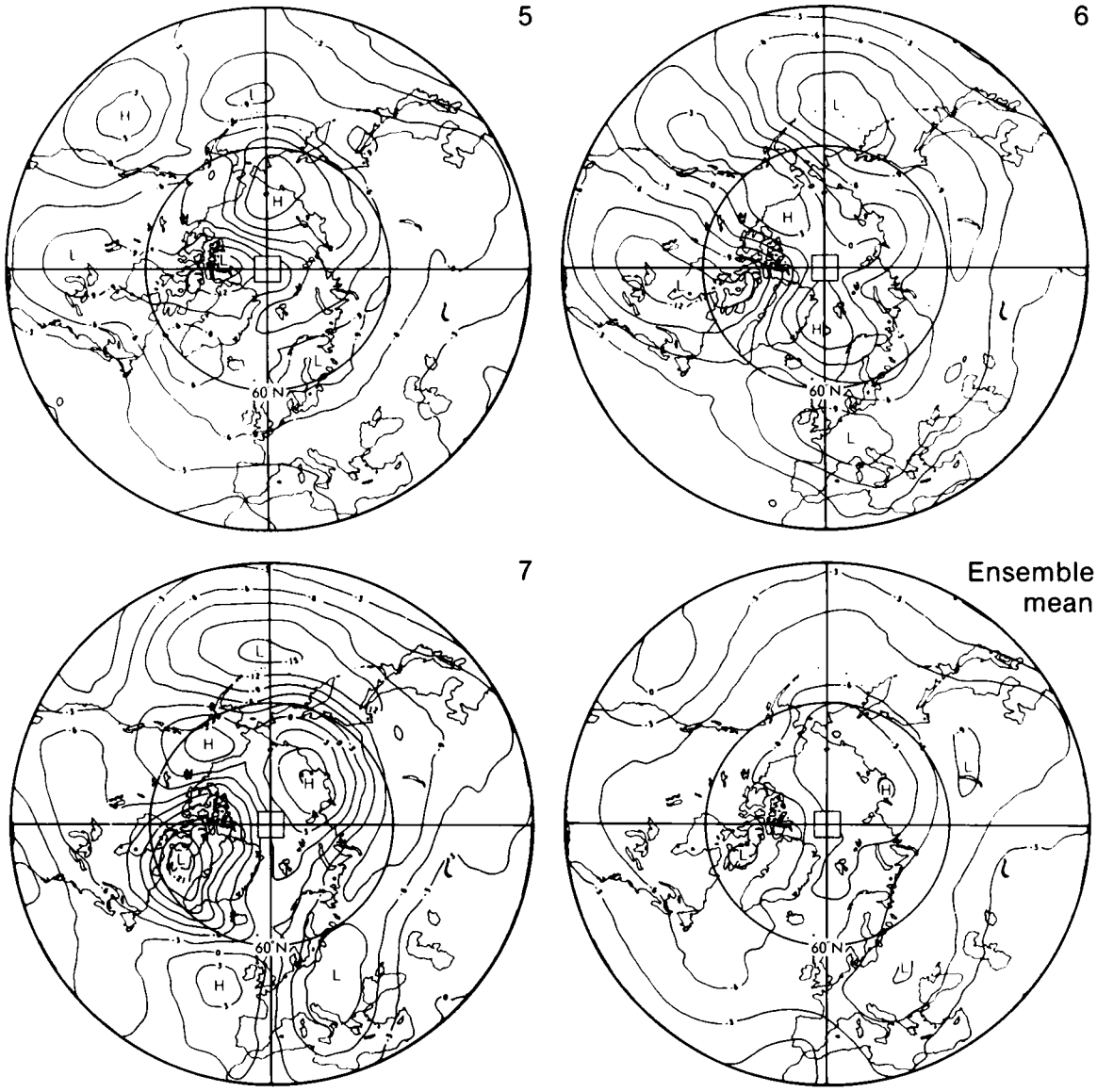

Figure 6 continued. Individual (from integrations 5–7) and ensemble-mean forecast 500 mb geopotential height anomaly (dam) for 3–17 October 1985.

up in terms of objective skill. Nevertheless, it is certainly encouraging that the actual pattern seems to bear a notable subjective resemblance to that which defines one of the two subsets predicted by the ensemble forecast.

The question arises as to whether the clustering can be traced back to earlier stages of the forecast. In the preceding period, 23 September–2 October, a similar pattern was again evident in integrations 5–7, it being displaced somewhat to the west in the sub-ensemble mean (not shown). Integrations 1–4 again show no sign of this PNA-like pattern.

Table II. *As Table I but with forecast divided into successive pentad means*

Integration	Forecast period						
	16–20 Sept. (day 1–5)	21–25 Sept. (day 6–10)	26–30 Sept. (day 11–15)	1–5 Oct. (day 16–20)	6–10 Oct. (day 21–25)	11–15 Oct. (day 26–30)	16–20 Oct. (day 31–35)
1 (00 GMT 12 Sept.)	0.31	0.03	0.21	0.10	−0.03	−0.01	−0.05
2 (12 GMT 12 Sept.)	0.47	0.02	0.01	0.03	−0.08	0.11	−0.17
3 (00 GMT 13 Sept.)	0.44	0.07	0.24	0.26	−0.21	0.05	0.05
4 (12 GMT 13 Sept.)	0.73	0.22	0.22	0.08	−0.19	0.03	−0.11
5 (00 GMT 14 Sept.)	0.75	0.40	0.34	0.27	0.23	0.04	−0.25
6 (12 GMT 14 Sept.)	0.82	0.46	0.28	0.06	0.23	−0.07	−0.10
7 (00 GMT 15 Sept.)	0.82	0.30	0.34	0.07	−0.02	0.10	0.08
1–7 average individual forecast	0.62	0.21	0.23	0.12	−0.01	0.04	−0.08
1–7 ensemble-mean forecast	0.73	0.30	0.32	0.16	−0.01	0.05	−0.10

Fig. 8 illustrates the development of differences between the sub-ensemble means 5–7 and 1–4 during the first 10 days of the forecast. Even at day 1 there is a low centre in the Pacific with a downstream high off the coast of North America and a further low to the north-east. Although the day 1 difference shows other features just as pronounced as these, the important point is that the aforementioned pattern remains more or less stationary throughout the first 10 days, whereas other areas of difference shift their position and disappear after a few days. This suggests that, while these latter differences are due to transient systems, the pattern in the Pacific/North American area seems to represent a genuine difference in the quasi-stationary large-scale circulation, implying that the migration of integrations 5–7 into a separate cluster can be traced right back to the initial conditions.

To demonstrate such behaviour objectively would require a method of cluster analysis, possibly based on a criterion of maximizing the phase correlation between cluster members rather than the more conventional one of minimizing the r.m.s. difference. It is intended to develop such a method to aid the investigation of this intriguing phenomenon in future long-range ensemble forecast experiments.

5. Conclusions

Having demonstrated the potential of the ensemble forecast technique to increase long-range predictability using a perfect-model approach, attempts at producing real-time operational monthly forecasts using a global 11-level climate model have commenced in the Synoptic Climatology Branch. The first such experiment was carried out for the operational long-range forecasting conference on 17 September 1985, for which an ensemble of seven integrations, initiated from consecutive analyses at 12-hour intervals between 00 GMT on 12 September 1985 and 00 GMT on 15 September 1985, was produced. The results show that all the individual model forecasts retain a small degree of skill out to 20 days, and the ensemble-mean forecast improves somewhat on the average individual forecast skill over this period.

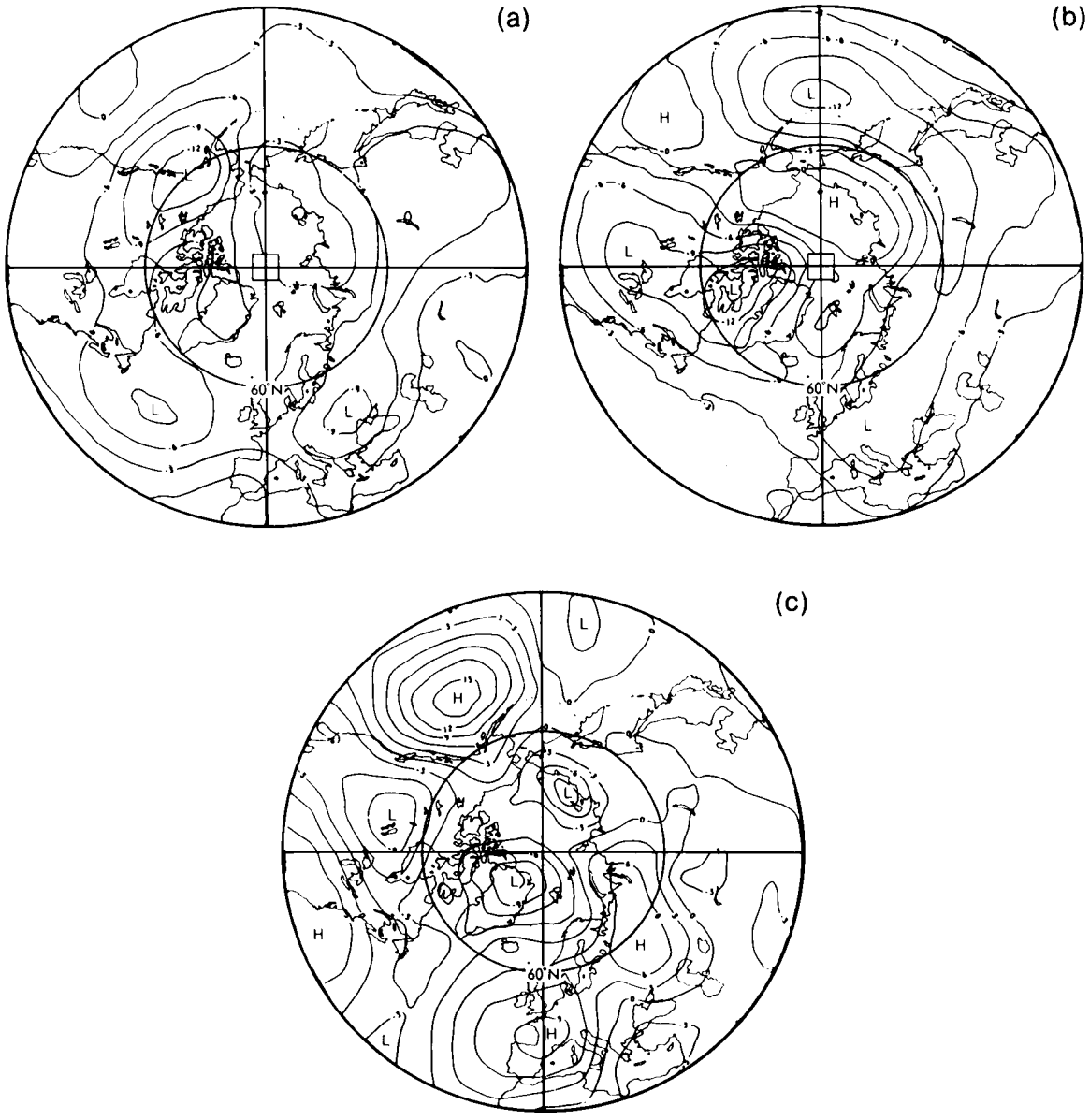

Figure 7. 500 mb geopotential height anomaly (dam) for 3–17 October 1985: (a) sub-ensemble-mean forecast formed from integrations 1–4, (b) sub-ensemble-mean forecast formed from integrations 5–7 and (c) observed.

An interesting feature concerns the apparent splitting of the integrations into two distinct clusters with respect to the forecast circulation patterns for the Pacific/North American region. This is most noticeable during the later part of the forecast, at which point the actual atmospheric pattern in the area bears some resemblance to one of the cluster patterns, but the development of the clustering may be traced back to the initial stages of the forecast. If typical of the manner in which ensemble forecast

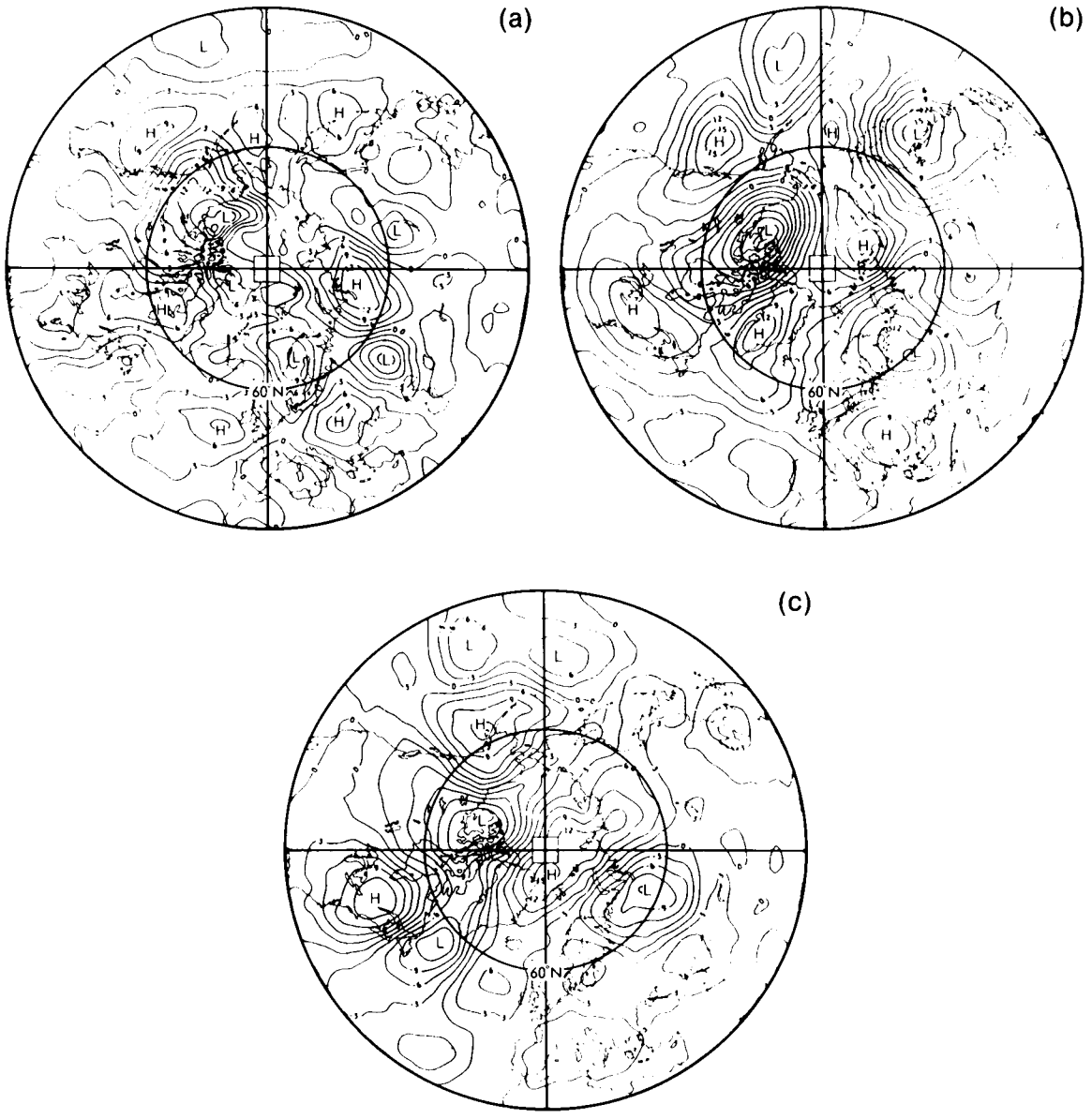

Figure 8. 500 mb geopotential height difference (dam) between the sub-ensemble mean of integrations 5–7 and 1–4: (a) forecast day 1, (b) forecast day 6 and (c) forecast day 10.

distributions evolve, such behaviour would have important implications for the interpretation and presentation of long-range ensemble forecasts in terms of probabilistic estimates of the occurrence of certain configurations of the quasi-stationary waves in the atmosphere. It is anticipated that these real-time ensembles of forecasts will be run at least once a quarter and will have a major impact on the operational requirements of the Synoptic Climatology Branch.

References

Bengtsson, L. and Simmons, A.J.	1983	Medium-range weather prediction — operational experience at ECMWF. *In* Hoskins, B.J. and Pearce, R.P. (eds): Large-scale dynamical processes in the atmosphere. London, Academic Press.
Corby, G.A., Gilchrist, A. and Rowntree, P.R.	1977	United Kingdom Meteorological Office five-level general circulation model. *Methods Comp Phys*, **17**, 67–110.
Folland, C.K. and Woodcock, A.	1986	Experimental monthly long-range forecasts for the United Kingdom. Part I. Description of the forecasting system. *Meteorol Mag*, **115**, 301–318.
Lorenz, E.N.	1982	Atmospheric predictability experiments with a large numerical model. *Tellus*, **34**, 505–513.
Mansfield, D.A.	(1986)	The skill of dynamical long-range forecasts, including the effect of sea surface temperature anomalies. (Submitted to *Q J R Meteorol Soc.*)
Marvon, R.H. and Storey, A.M.	1985	A multivariate statistical model for forecasting anomalies of half-monthly mean surface pressure. *J Climatol*, **5**, 561–578.
Murphy, J.M.	1985	The impact of ensemble forecasts on predictability. (Unpublished, copy available in the National Meteorological Library, Bracknell.)
Shukla, J.	1981	Dynamical predictability of monthly means. *J Atmos Sci*, **38**, 2547–2572.
Slingo, A.	1985	Handbook of the Meteorological Office 11-layer atmospheric general circulation model. Volume 1: Model description. (Unpublished, copy available in the National Meteorological Library, Bracknell.)
Wallace, J.M. and Gutzler, D.S.	1981	Teleconnections in the geopotential height field during the northern hemisphere winter. *Mon Weather Rev*, **109**, 784–812.

551.515.4(46):551.509.326

The Spanish plume — testing the forecaster's nerve

By R.M. Morris

(Assistant Director (Central Forecasting), Meteorological Office, Bracknell)

Summary

An example is described of a spectacular development of thunderstorms arising out of dynamical interaction between a typical mid-latitude upper cold trough and a reservoir of hot air over Iberia. Prediction of the development by the Meteorological Office 15-level numerical fine-mesh model is also described.

1. Introduction

Experienced forecasters will all agree that the most difficult weather situations to predict with any accuracy are those in which development is a feature of the evolution rather than translation of existing weather. One weather situation which readily falls into this category is the development over Iberia and western France of widespread thunderstorms which spread to the United Kingdom. This weather pattern, which usually occurs at least once or twice during the summer months between May and September, is known as the 'Spanish plume'. A good example of this phenomenon occurred during 19 and 20 May 1986 and, despite the fact that the evolution was extremely well forecast by the Meteorological Office operational numerical weather prediction model, the writer is aware that some forecasters were very sceptical of the predicted evolution at the time. For this reason alone it seems very desirable that the Spanish plume should be documented in the literature as a lesson for the unwary and for inexperienced forecasters of the future.

2. Mechanics of the development

The main conditions for development of a Spanish plume include an upper trough slowly advancing towards Biscay and Iberia, and a zone of strong temperature gradient in the lower troposphere over Iberia. The baroclinic zone on the forward side of the upper trough is usually identified with a moderately active cold front whilst the baroclinic zone over Iberia is initially dynamically inactive. As the upper trough advances towards Iberia a number of dynamical forces come into play (see Fig. 1). These can be deduced subjectively using the quasi-geostrophic omega equation to link vertical motion to the thermal and vorticity advection (see, for example, Morris 1972). The pre-existing upper flow over Iberia takes up the cyclonic curvature of the encroaching flow and causes limited dynamical ascent and falling surface pressure over Iberia. This in turn causes thermal advection to develop within the baroclinic zone flanking the hot cell; in particular warm air advection causes enhancement of the dynamical ascent with further falls in surface pressure. The adjusting low-level wind creates cold air advection in the western coastal zone so that a well-marked discontinuity in thermal advection is created over Iberia with ascending air ahead of the sharpening thermal ridge and descending air to the rear; the Spanish plume is born.

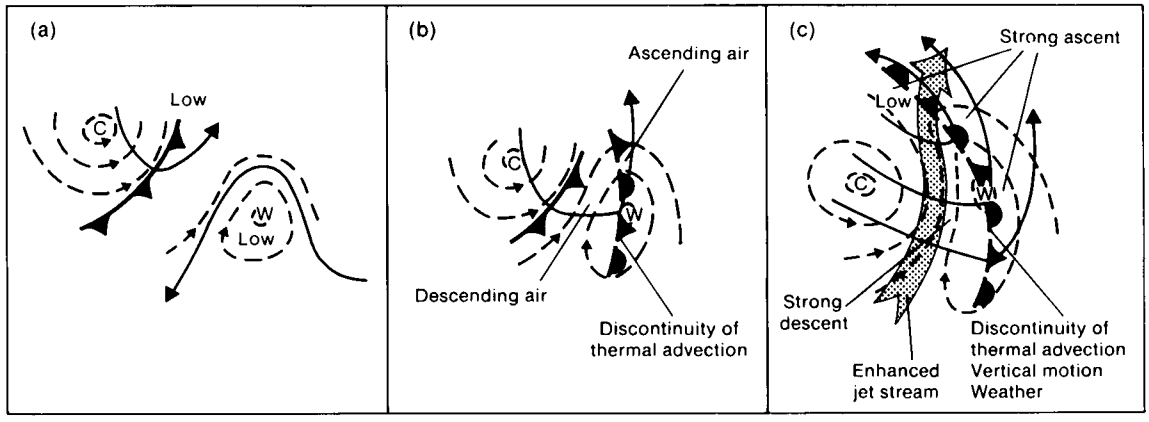

Figure 1. The development of the Spanish plume. Solid lines indicate surface flow, dashed lines thermal flow. For description of development see text.

From this point on the plume is capable of a quasi-independent dynamical evolution. However, the organization of the thermal wind on the forward side of the upper trough causes an intensification of the thermal gradient and an increase in wind strength aloft. This in turn intensifies the vorticity advection along with a corresponding increase in the magnitude of vertical motion on the forward side of the trough. (Often there is an enhanced cold exit region to the south-south-west jet with associated cyclogenesis and widespread precipitation.) The plume effectively becomes the main frontal zone and the old cold front associated with the upper trough tends to lose its identity under the influence of the adjusting dynamical forces.

3. An example: 19 and 20 May 1986

Using initialized fields from the Meteorological Office numerical weather prediction 15-level fine-mesh model, Figs 2(a), (b) and (c) depict the synoptic situation at 00 GMT on 19 May 1986. Fig. 2(a) is a composite of the mean-sea-level pressure (mslp) and 850 mb wet-bulb potential temperature (θ_w). Note the zone of strong θ_w gradient over north France, Biscay and Iberia and also the weak gradient

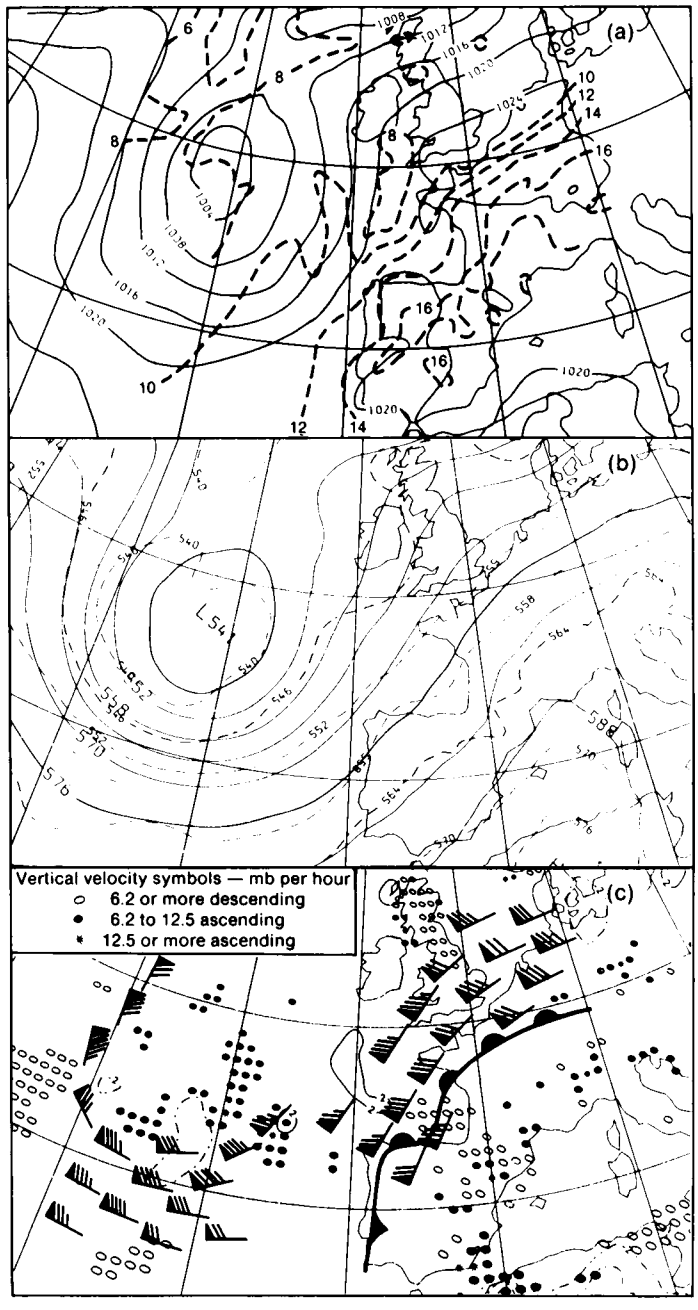

Figure 2. The synoptic situation at 00 GMT on 19 May 1986: (a) mean-sea-level pressure (mb) (solid lines) and 850 mb wet-bulb potential temperature (°C) (dashed lines), (b) 500 mb geopotential height (dam) (solid lines) and 500–1000 mb thickness (dam) (dashed lines) and (c) composit showing maximum winds, warm edge of 850 mb wet-bulb potential temperature, vertical velocity (see key) and thermal advection (°C per 6 hours) (solid lines, warming, dashed lines, cooling). In (c) vertical velocity and thermal advection are each meaned over the 850–500 mb layer.

associated with an Atlantic cold front. Fig. 2(b) is a composite of the 500 mb geopotential height and 1000–500 mb total thickness — note the broad zone of thermal gradient from the vortex to Iberia and France. A composite consisting of the maximum wind, thermal advection and vertical velocity (the latter two each meaned over the 850–500 mb layer) is shown in Fig. 2(c). The warm edge of the 850 mb θ_w gradient (denoted by frontal symbols) is also included for completeness. At this stage the main dynamical ascent is closely associated with the strongest flow flanking the upper vortex. The composite is a diagnostic analysis of the type prepared daily as an experiment in the Central Forecasting Office (CFO) at Bracknell with the objective of displaying the most essential dynamical functions on one chart to explain cause and effect in the distribution of weather. Developments in the troposphere over western Europe during the subsequent 36 hours will be largely illustrated by composites of the format depicted in this figure.

Fig. 3(a) illustrates the dynamical situation at 12 GMT on 19 May. The upper trough has advanced closer to Iberia whilst downstream the jet axis has been transferred north across the United Kingdom and has weakened somewhat. Ascending air is now more widespread over Iberia, and both warm and cold air advection is in evidence in this region. Note that the warm air advection over south-west Britain is not associated with any significant ascent (i.e. $\geqslant$6.2 mb per hour) due probably to lack of support from the vorticity advection aloft. Strong ascent is evident west of Ireland in the cold exit region of the south-south-west jet. Fig. 3(b) depicts the distribution of cloud at 1200 GMT derived from Meteosat; significant weather reported at the surface is also shown. At this time there was a band of high cloud across Iberia but no evidence of cumulonimbus activity. It was this picture which gave rise to the scepticism. Six hours later Meteosat revealed quite a different picture (Fig. 3(c)) while considerable convective cloud and thunderstorms were reported in northern Spain.

Fig. 4(a) depicts the dynamical situation at 00 GMT on 20 May. Ascent is now indicated widely over south-west Britain and a further broad area of ascent appears centred just to the north-west of Iberia. There are warm air advection fields in both regions and positive vorticity advection is probably contributing to ascent just to the rear of the upper ridge axis (north) and ahead of the upper trough axis (south). The rapid northward advance of rain and thunderstorms to north-west France is revealed in Fig. 4(b) although there is a curious phase difference between this and the model analysis of ascending air to the north. This aspect will be discussed further in section 4. As Fig. 4(c) shows, the thundery rain has spread to most of England by 06 GMT.

By 12 GMT on 20 May cold air advection is broadly established across Biscay and extreme western France with warm advection covering eastern Britain and the North Sea (Fig. 5(a)). Ascending air extends broadly from north-east Spain across north France to Scotland. Note the increase in strength of the maximum wind on the forward side of the advancing upper trough. Fig. 5(b) illustrates the distribution of cloud and significant weather for the same time. By this stage the old cold front is dynamically inactive, thermally weak and without evidence of any significant weather.

4. The numerical model forecast

The characteristics of the Meteorological Office 15-level numerical weather prediction model were described in special issues of the *Meteorological Magazine* recently (Meteorological Office 1985a, b). The fine-mesh T+12-, T+24- and T+36-hour forecasts of mslp and instantaneous local rainfall rates, based upon initial conditions at 00 GMT on 19 May, are shown in Figs 6(a), (b) and (c). The main features of the evolution were very well predicted with the only significant error being the timing of the movement of rain across northern England and southern Scotland during the first 24 hours. Figs 7(a), (b) and (c) depict the corresponding forecasts of vertical motion and thermal advection. It is interesting to see how the T+24- and T+36-hour fields look slightly more consistent with the observed significant

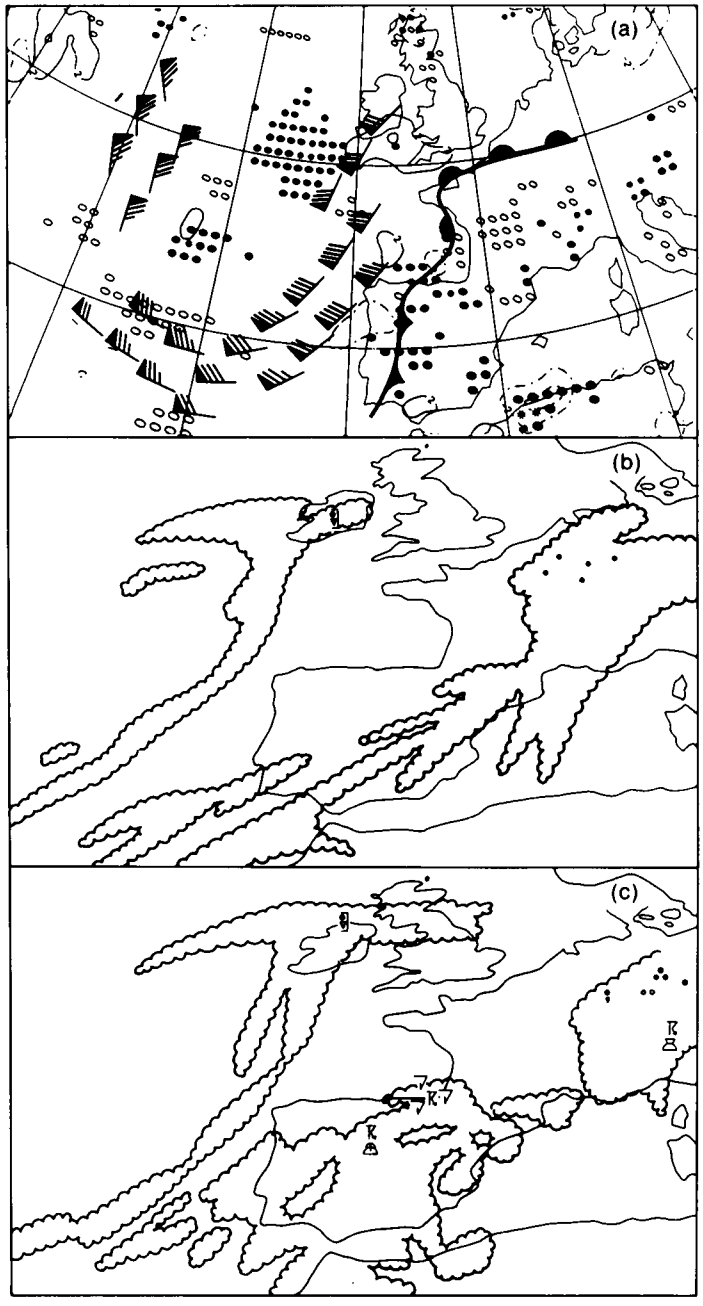

Figure 3. (a) Same as Fig. 2(c) but for 12 GMT on 19 May 1986, (b) distribution of cloud at 12 GMT on 19 May 1986 derived from Meteosat, and significant weather reported at the surface for the same time and (c) as (b) but for 18 GMT.

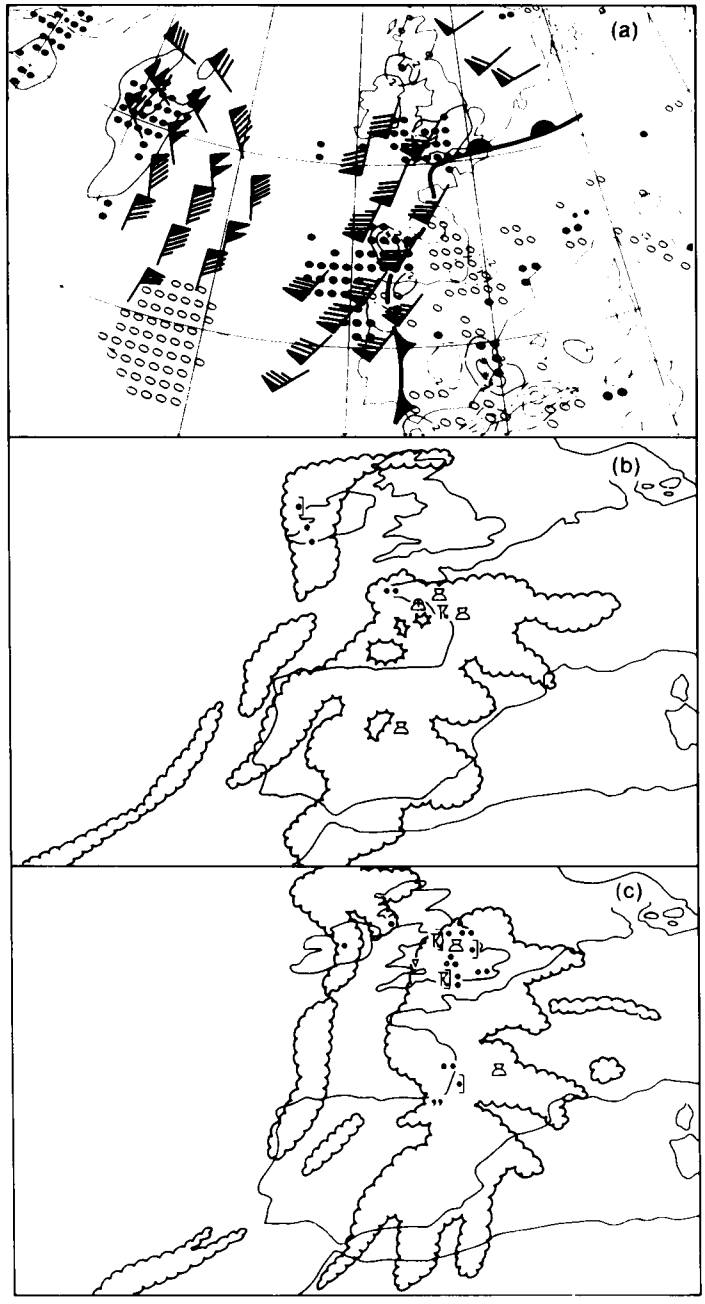

Figure 4. Same as Fig. 3 but for 00 GMT on 20 May 1986 ((a) and (b)) and 06 GMT on 20 May 1986 (c).

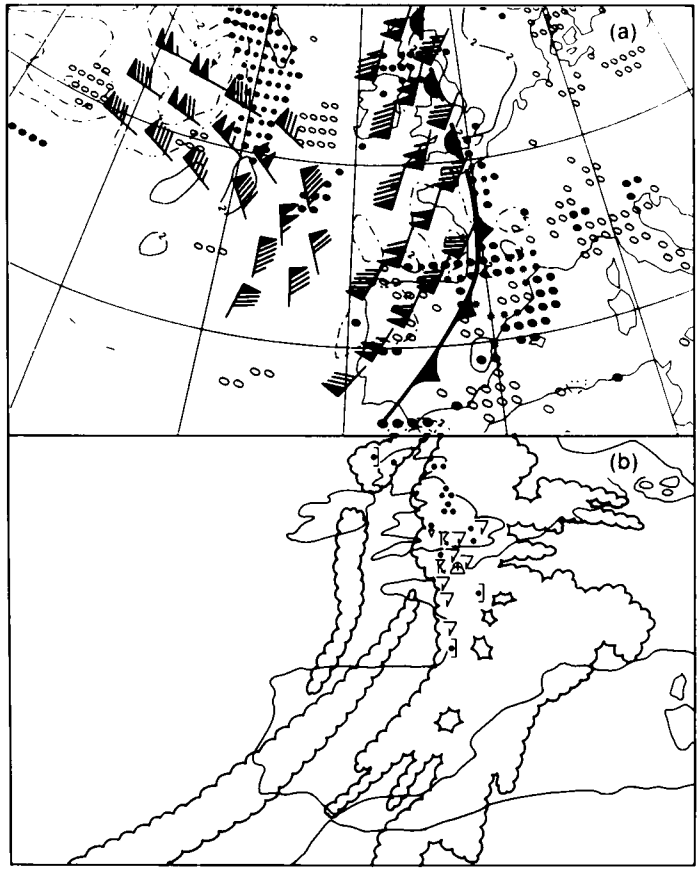

Figure 5. (a) Same as Fig. 3(a) but for 12 GMT on 20 May 1986 and (b) same as Fig. 3(b) but for 12 GMT on 20 May 1986.

weather than the corresponding analysis fields (Figs 4(a) and 5(a)). There is a possible explanation for this; the assimilation of fresh data is quasi-continuous in the model analysis scheme and so the solutions to the equations are constrained by the need to fit real observations at the main analysis times. This can introduce spurious solutions locally for variables that are not directly observed. The forecasts are not so constrained, however, and smoother, dynamically more consistent solutions should be obtained.

One of the most useful new products derived from the fine-mesh operational suite is the distribution of convective cloud tops (see Davies 1986). Fig. 8 depicts the T+36-hour forecast verifying at 12 GMT on 20 May. Most of the cumulonimbus cloud tops in the thundery area were forecast to be above a flight level of 30 000 ft (FL 300) with several places above FL 350 and one point in south-east England above FL 400. This output is used operationally by the International Civil Aviation Organization Regional Area Forecast Centre located within CFO.

5. Concluding remarks

One of the most significant aspects of this case is the way in which the evolution is amenable to human perception using quasi-subjective reasoning. Even without the benefit of modern numerical models the discerning forecaster could expect some development of a weather system to occur between Iberia and southern England. Of course there would be doubts — would the ascent of air be enough, would the air

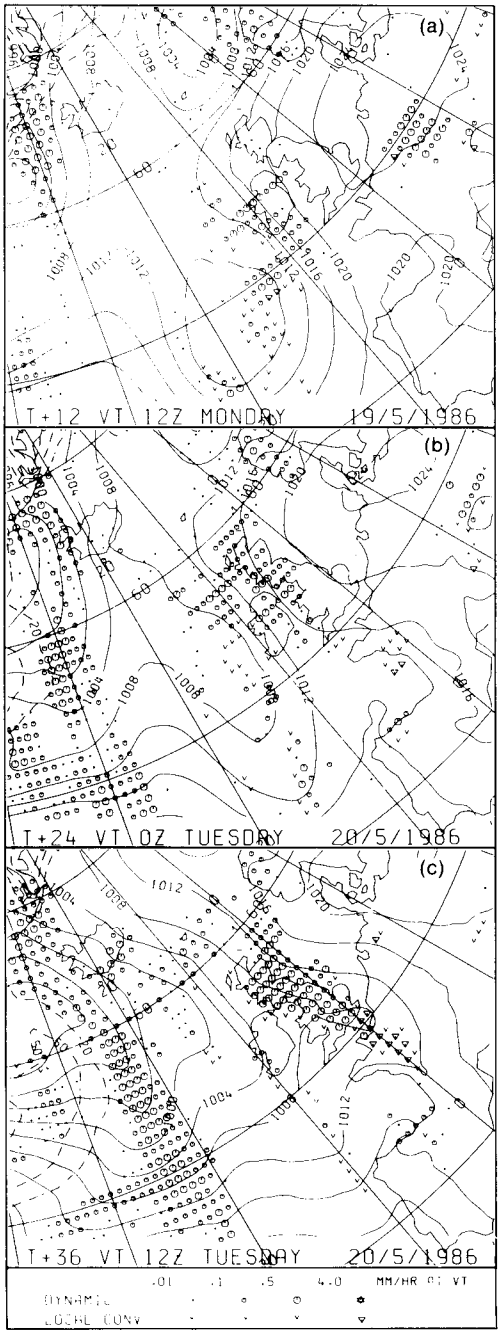

Figure 6. Fine-mesh 15-level numerical model forecast of mean-sea-level pressure (mb) (solid lines) and rainfall (see key) for (a) T+12, (b) T+24 and (c) T+36 hours, all based upon data time 00 GMT, 19 May 1986.

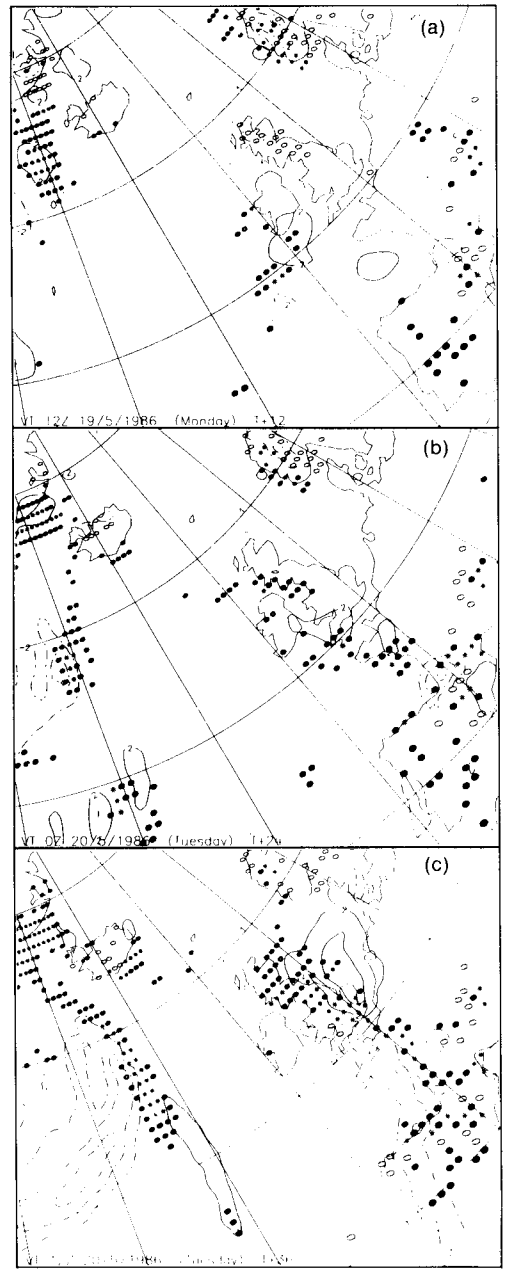

Figure 7. Fine-mesh 15-level numerical model forecast of vertical velocity and thermal advection (see Fig. 2 for key) for (a) T+12, (b) T+24 and (c) T+36 hours, all based upon data time 00 GMT, 19 May 1986.

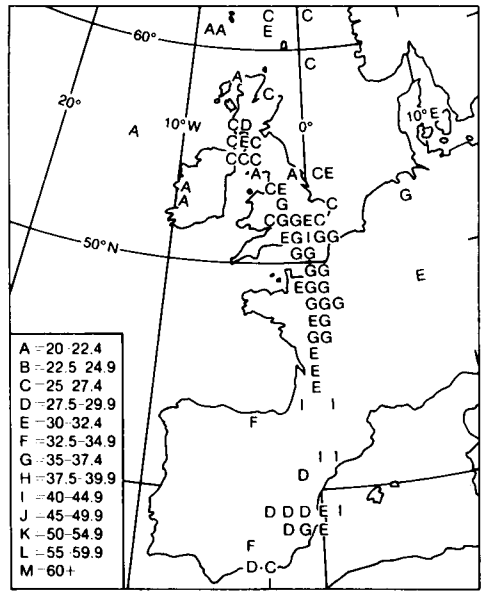

Figure 8. Fine-mesh 15-level numerical model T+36-hour forecast of convective cloud tops above 20 000 ft (key gives heights in thousands of feet) for 12 GMT on 20 May 1986.

be sufficiently moist and would the air be convectively unstable? It is these aspects that test the forecaster's nerve, given the innocuous weather conditions prevailing at the time he has to make up his mind. The ability of the 15-level numerical model to predict the evolution so successfully should increase the forecaster's confidence, but model forecasts are not always so accurate (for a variety of reasons, e.g. poor analysis in some crucial areas) — why otherwise did some forecasters doubt the predicted evolution? In such cases the successful forecaster, who doesn't lose his nerve, is the one who uses his discerning and perceptive logic to understand how the numerical model has produced its solution.

Browning and Hill (1984) describe a mesoscale convective system which, if not exactly the same, looks very similar in development to the example discussed here. It would be interesting to see how the current numerical model, with the range and versatility of output described here, would predict the evolution of that system.

References

Browning, K.A. and Hill, F.F.	1984	Structure and evolution of a mesoscale convective system near the British Isles. *Q J R Meteorol Soc*, **110**, 897–913.
Davies, T.	1986	Convective cloud forecasts from the Meteorological Office fine-mesh model. *Meteorol Mag*, **15**, 371–372.
Meteorological Office	1985a	Operational numerical forecasting: models and products. *Meteorol Mag*, **114**, 221–251.
	1985b	Operational numerical forecasting: evaluation and applications. *Meteorol Mag*, **114**, 253–291.
Morris, R.M.	1972	The trowal, an important feature of frontal analysis. *Meteorol Mag*, **101**, 150–153.

551.526.6:551.465.7

Ocean and atmosphere interact!

By S.J. Foreman

(Meteorological Office, Bracknell)

Summary

A brief description is given of the coupled ocean–atmosphere model developed by the Dynamical Climatology Branch of the Meteorological Office. Some characteristics of the first experiment performed with this model are discussed.

1. Introduction

The Dynamical Climatology Branch of the Meteorological Office uses numerical models of the atmosphere to simulate the climate. One of the strongest constraints on the atmosphere is its interaction with the oceans through the sea surface temperature (SST). To date, SSTs have been specified from observations for investigations of present-day climate. However, for studies of climate change, it has been necessary either to impose arbitrary perturbations of the SSTs, or to use a simple heat balance model of the upper layers of the ocean. Clearly such procedures are unsatisfactory if, as often happens, it is suspected that the climate to be modelled differs markedly from that of the present day. In these circumstances a better approach would be the simulation of SSTs using an explicit calculation of the ocean circulation during the integration of the atmosphere model. This is now possible using a general circulation model for the oceans which has been developed in recent years.

2. The models

(a) *Atmosphere*

The 11-layer model, as its name implies, calculates values of atmospheric variables (temperature, humidity, winds) for 11 layers in the vertical (using pressure divided by surface pressure as the vertical coordinate) on a uniform $2.5 \times 3.75°$ latitude–longitude horizontal grid; it is described in more detail by Slingo (1985). The model includes a comprehensive 'physics' package similar to that of the operational fine-mesh model. Synoptic features are resolved by the 11-layer model, which produces realistic simulations of the present-day climate. Adjustments of the atmospheric circulation to changes in the SSTs occur over time-scales of the order of months.

(b) *Ocean*

The ocean model is based on that of Bryan (1969) and produced by Cox of the Geophysical Fluid Dynamics Laboratory, Princeton (Cox, personal communication), though it has been extensively modified to allow it to run alongside the atmosphere model. In the form used for the experiment described below, the model has 12 layers in the vertical and uses the same horizontal grid as the atmosphere model. It calculates values for the current velocity, temperature and salinity (which strongly influences the density) of the water by solving the equations of motion, and the equations describing the conservation of heat and salt. These are solved using numerical techniques similar to those used in atmosphere models. Eddies in the ocean are more than an order of magnitude smaller than anticyclones and depressions, their counterparts in the atmosphere. As the model is unable to resolve these eddies it is necessary to include strong lateral diffusion. Time-scales in the ocean are much longer than in the atmosphere, so that the upper layers of the ocean take tens of years to reach equilibrium with changes in

the surface forcing, while in the deep oceans this process may take millennnia. Ocean simulations must therefore be run for much longer periods than atmospheric ones if equilibrium is to be attained.

(c) *Coupling of the models*

The two models are coupled through their interactions at the sea surface. Wind stress and fluxes of sensible and latent heat are calculated by the atmosphere model and passed to the ocean model for use at its upper boundary, as are the radiative fluxes and the amounts of precipitation and evaporation. These quantities are accumulated during 5 days of integration of the atmosphere model, and then passed to the ocean model which uses them as boundary conditions for the same 5 days. Calculated ocean model temperatures for the top model layer are then passed back to the atmosphere model, and are used as the SSTs for the following 5 days. This cycle continues throughout the simulation, and is illustrated in Fig. 1.

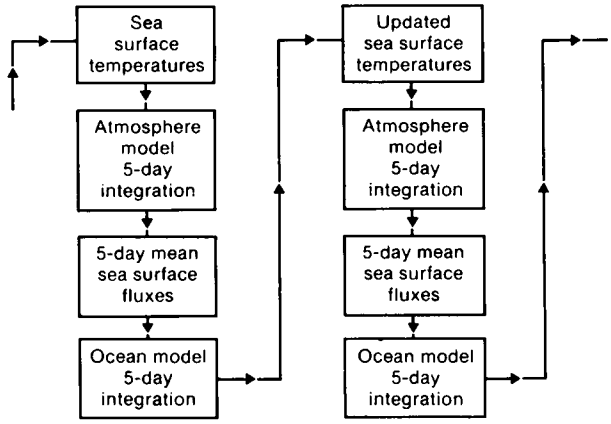
Sea surface temperatures
Atmosphere model 5-day integration
5-day mean sea surface fluxes
Ocean model 5-day integration
Updated sea surface temperatures
Atmosphere model 5-day integration
5-day mean sea surface fluxes
Ocean model 5-day integration

Figure 1. Schematic diagram of the integration cycle for the coupled model.

This process would be too expensive to run to equilibrium. Instead, a technique known as 'asynchronous coupling' is used. In this the ocean and atmosphere models are run coupled as above for a number of years ('synchronous coupling') during which the fluxes at the ocean surface calculated by the atmosphere model are stored. The ocean model is then run using this forcing for several more years, following which the two models are again run synchronously. Since this approach accelerates the system's approach to equilibrium and the ocean model requires fewer resources than the atmosphere model this process makes it possible to run to a steady climate.

A further complication which arises is the treatment of sea ice. A comprehensive sea-ice model is being developed, but was not ready in time to be included in the first experiment using the coupled ocean–atmosphere model. Therefore, climatological sea-ice extents have been used instead.

3. A preliminary experiment

A preliminary experiment, to run the coupled model synchronously for 18 months, has been initiated. This was started from atmospheric data for the last day of April derived from a previous 'atmosphere-only' simulation of the present-day climate which used climatological SSTs, and the quasi-equilibrium state of an 'ocean-only' experiment which used annual mean climatological forcing at the sea surface. The two were merged at the start of the integration; the initial temperatures for the top ocean layer were taken from an appropriate climatology to remove gross differences between the ocean annual mean simulation and the seasonal climatology.

As the coupled system would take about 10 years to reach a near-equilibrium state for the atmosphere and upper layers of the ocean, and far longer for the deep ocean, the present experiment can only be expected to indicate trends in the evolution of the coupled system.

Interaction between the two models takes place at the sea surface. Inevitably, fluxes calculated by the atmosphere model will differ from climatological fluxes, resulting in modifications to the ocean circulation when compared with climatology; likewise the SSTs calculated by the ocean model will not be the same as those derived from climatology, so modifying the atmospheric flow. As a result it should be expected that the simulations of ocean and atmosphere would differ from those obtained using climatological fluxes and SSTs. The simulated SSTs are subject to both the dynamics of the ocean model and to the atmospheric forcing, and therefore provide a suitable indication of the behaviour of the coupled system.

Simulated and observed distributions of SST for the winter months (December, January, February), after 10 months' simulation, are shown in Fig. 2. The coupled model maintains the general pattern of

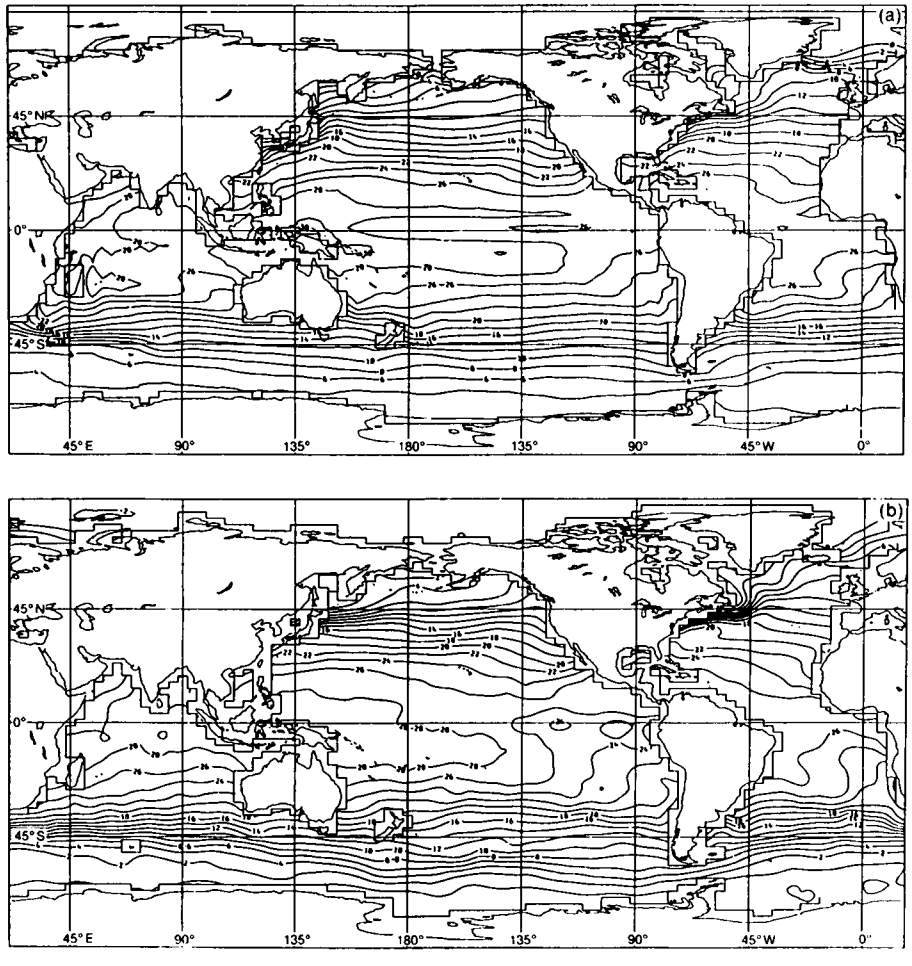

Figure 2. Sea surface temperatures (°C): (a) the coupled model experiment and (b) climatology (from Levitus 1982) for the winter months (December, January, February).

SST, including the minimum along the equator, and the contrast between the warm water in the west of the tropical oceans and the cooler water in the east. Certain errors are apparent, however. For example, the water along the equator is too cold in the Atlantic, Indian and western Pacific oceans; these errors are being investigated further using a high-resolution tropical Pacific model. Also areas of ocean upwelling off the western coasts of continents tend to be too warm, notably near Peru and western north Africa, while western boundary currents are too cool due to the coarse resolution of the ocean model. In the southern hemisphere the mid-latitude SSTs tend to be too cool as a result of the thick top layer, which cannot represent the shallow mixed layer (a feature also found in the northern hemisphere during its summer) and at higher latitudes the SSTs are too warm as a result of deficiencies of the initial conditions used for the ocean. Gradients are too weak as a result of the strong lateral diffusion used in the ocean model.

4. Future developments

The present experiment has proved that the system for running the coupled model works, and has indicated areas in which improvements in model formulation are necessary. Further experiments will be performed during the next year which will use a version of the ocean model with higher resolution in the vertical to enable the mixed layer to be represented and start from ocean conditions derived from seasonally varying forcing. The interactive sea-ice model should also be available. In addition to the simulation of the present-day climate necessary to validate the results from the models, perturbation experiments to investigate the climatic aspects of increased atmospheric carbon dioxide are planned.

5. References

Bryan, K.	1969	A numerical method for the study of the circulation of the world ocean. *J Comput Phys*, **4**, 347–376.
Levitus, S.	1982	Climatological atlas of the world ocean. NOAA Prof. Paper No. 13.
Slingo, A.	1985	Handbook of the Meteorological Office 11-layer atmospheric general circulation model. Volume I: Model description. (Unpublished, copy available in the National Meteorological Library, Bracknell.)

551.593.653(4)

Noctilucent clouds over western Europe during 1985

By D.M. Gavine

(Leith Nautical College, Edinburgh)

Table I summarizes noctilucent cloud (NLC) reported to the Aurora Section of the British Astronomical Association (BAA) during 1985, from Finland (F), Denmark (D), Great Britain (G), one experienced observer, Mr van Loo, at Ittegem, Belgium (B), and Mr Kaye at the meteorological station in Detmold, Federal Republic of Germany. Also received was a list of positive sightings from Alberta, Canada, by Mr Zalcik, Mr Brown and Mr Kushniryk.

Times (UT) in the second column of the table are of reported sightings, not necessarily the duration of a display. Maximum elevations of the upper border are given, with limiting azimuths where possible. Coordinates of the observing stations are given to the nearest half-degree. No routine hourly reports of sky cover are now received from meteorological stations, so estimates of the 'negative' nights, (i.e. clear

or slight cloud with no visible NLC) are based on prolonged watches by experienced amateur observers.

Contributions to the year's survey were received from 17 British amateur observers and 6 meteorological stations. There are now four regular observers in Denmark, co-ordinated by Mr J.Ø. Olesen; their colour photographs, especially of panoramas of major displays, are of a very high standard and have been exhibited at BAA meetings. The Finnish network, whose reports are compiled by Mr V. Mäkelä, now has 24 observers spread widely over the country, their data being handled by microcomputer. The Section is very much indebted to Finland's highly efficient and enthusiastic team, which now has plans to encourage NLC observing in neighbouring countries.

Of a total of 42 definite NLCs reported over Europe, 26 were seen in Finland, 14 in Britain, 10 in Denmark, 2 in Belgium, and in addition 10 displays and one 'suspect' were observed in Alberta. In one of the worst summers this century, Britain suffered very badly from tropospheric cloud, and the fact that NLC was visible on so many of the clear nights may indicate a high incidence of the phenomenon in 1985. No parallactic photography was possible because of cloud.

The statistics reveal a curious anomaly between the occurrence of NLC in the United Kingdom/Denmark and in Finland. From mid-May up to 4/5 July only two displays were seen in Finland despite a relatively quiet geomagnetic field, and in this period there were 32 negative nights; yet in the same period Britain and Denmark experienced 12 displays, 4 of them major. Finnish observers then continued to see NLC frequently until 16/17 August, with two suspect appearances in the last week of that month.

The Aurora Section offers thanks to all observers, amateur and professional, for helping to keep the survey going in the interests of continuity of data, to the staff of the Department of Meteorology, University of Edinburgh for forwarding reports, and to Dr Michael Gadsden (University of Aberdeen), Mr Ron Livesey (Director, BAA Aurora Section) and Mr Neil Bone (Aurora Director, Junior Astronomical Society) for helpful collaboration.

Immediate NLC news is announced in *The Astronomer* monthly magazine. Instructions for observing NLC, and report forms, may be obtained from the Section Assistant Director, Dr D.M. Gavine, 29 Coillesdene Crescent, Edinburgh, EH15 2JJ.

Table I. *Displays of noctilucent clouds over western Europe during 1985*

Date night of	Times UT	Notes	Station position (to nearest 0.5 degree)	Time UT	Max elev.	Limiting azimuths
					degrees	
5 6 May		No NLC (F)				
6 7	2340–0105	Faint veil and bands at Kuopio.	63° N 27.5° E	2340	20	090 150
				2350	22	100 170
7 8 to 8 9		No NLC (F)				
9 10	2330–0105	Medium bright veil and bands at Kuopio, reddish-white, suspect NE movement.	63° N 27.5° E	2330	No NLC	
				2350	20	125 240
				0015	24	125 250
				0055	54	105 210
				0105	NLC suspect	
12 13 to 14 15		No NLC (F)				
15 16	2300–0005	Faint bands and billows at Kuopio, no NLC at Helsinki.	63° N 27.5° E	2300	No NLC	
				2340	16	010 035
				2350	13	010 035
				0005	NLC suspect	

Date night of	Times UT	Notes	Station position (to nearest 0.5 degree)	Time UT	Max elev.	Limiting azimuths
					degrees	
16–17 to 17–18		No NLC (F)				
20–21		No NLC (F)				
26–27 to 27–28		No NLC (F)				
28–29 to 30–31		No NLC (B, F)				
31 May to 3–4 June		No NLC (B, F, G)				
4–5 to 6–7		No NLC (B, F)				
8–9		No NLC (B, D)				
9–10		No NLC (D, F)				
10–11		NLC in Alberta. No NLC (F).				
11–12		No NLC (F)				
12–13		No NLC (G)				
13–14	2214–2307	Faint bands and NLC patches at Helsinki, very faint bands visible with binoculars at Rønne.	60° N 24.5° E	2214	14	340–000
				2219	35	340–005
				2230	18	000–005
				2249	NLC suspect	
			55° N 14.5° E	2110	12	000–022
				2208	15	000–045
				2315	NLC suspect	
14–15	2217–0330	Bands, billows and whirls observed throughout Britain, Belgium, Denmark. Bands and billows in Alberta.	56° N 03° W	2340	8?	350
				2345	10?	340–350
				0000	15	015–040
				0015	20	Cloud–060
				0030	20	Cloud–090
				0045	NLC	Cloud
			56° N 04.5° W	2256–0035	15+	Cloud
			56° N 10° E	2233	13	288–008
				2330–2352	22	300–350
			55° N 01.5° W	2217	NLC trace	
			(Morpeth)	2235	30	330–052
				2245	24	336–046
				2300	20	345–050
			55° N 01.5° W (Newcastle)	0140–0330	80?	290–335
			55° N 14.5° E	2240–2250	12	315–045
			54.5° N 06° W	0005	5	060–078
				0025	5	058–076
			54° N 02.5° W	0145	10	000
			52° N 02° W	2230	8	340–030
			51° N 04.5° E	0135	9	346–072
				0155	9	347–072
				0215	8	348–070
15–16	2345–0245	Extensive display of pronounced billows, medium brightness, visible only in N Britain after cloud clearance.	57.5° N 03.5° W	2345	8	340–040
				0015	10	340–080
				0100	25	330–100
			56.5° N 03° W	0040	10	
			56° N 03° W	0130	45	010–100
				0140	80	000–100
				0150	100	000–100
			56° N 04° W	0100	12	350–050
				0110	12	Cloud–050
				0122	40	
				0130	60	Cloud
			55.5° N 04.5° W	0100–0130	19	355–090
			55° N 01.5° W	0130	36	336–086
				0145	50	332–120

Date night of	Times UT	Notes	Station position (to nearest 0.5 degree)	Time UT	Max elev degrees	Limiting azimuths
15 16 (contd)				0200	90+	
				0215	90+	158
				0245	Dawn	
16 17	2140–0100	Faint bands visible in trop. clouds, Britain, Denmark and Alberta. No NLC in N Finland.	56° N 03° W	2330	5°	315
				2345	4	000 030
				0005	4	340 030
				0030	5	000 035
			55.5° N 12.5° E	2140	15°	000–045
			55° N 01.5° W	0000	5	020 031
				0015	10	005 037
				0030	10	004 045
				0045	11	000 045
				0100	Low	Cloud
			52° N 00.5° W	0049	Low	045
17 18		Bands and billows at Edmonton (Alberta). No NLC (F).				
18 19	2333–0100	Very faint veil, possible band and billows, Scotland and N England. No NLC (F).	56° N 04° W	2333	10	
			56° N 03° W	0015	10	320 030
				0100	NLC suspect	
			53.5° N 03° W	0000	5	330 015
19 20	2220–0100	Billows and whirls at Kinloss, faint bands and patches in trop. cloud, S Scotland and N England.	57.5° N 03.5° W	0015	17	020 065
			57° N 04° W	0040 0100	20	015 045
			56° N 03° W	2245	30	330 000
				2320	15	330 020
				0000 0100	20	Cloud
			55° N 01.5° W	2220	40	
				2250	NLC flam	
				2320	46°	
				2325	10	326 047
20 21	2220–2250	Very faint parallel bands in haze at Morpeth. Faint bands at Edmonton. No NLC (F).	55° N 01.5° W	2220	44	320 070
				2235	43	060
				2240	38°	
				2250	No vis. NLC	
21 22		No NLC (F)				
22 23		No NLC (D, F)				
23 24	2215–0145	Bright display, all forms, observed in N England. Scotland overcast. No NLC (F).	55° N 01.5° W	2230	25	Cloud
				2325	8	336 018
				2340	7+	Cloud
				2355	8+	340 003
				0010	Cloud	
			54° N 01° W	0045	9	350
				0145	13	345
			53.5° N 03° W	2225	25	315
				2230	20	260 040
				2330	Low	270 030
			53.5° N 02° W	2215	20	000 020
				2230	20	310 320
				2300	10	
				2330	Cloud	
			53.5° N 01.5° W	2225	15	310 030
				2245	15	310 030
				2300	12	
				2315	9	350 020
				2345	5	000
24 25		No NLC (F)				
25 26	2215–0225	Moderately bright bands and whirls in N England, billow development about 0130. Faint bands at Jämsä, Finland. Major display at Edmonton all forms, very bright, alt. 90° at 0400 local time.	62° N 25° E	2215–2300	40	000 030
			54° N 01° W	2315	3	000 030
				2330	3	000 030
				2345	7	340 030
				0001	7	340 030
				0015	9	330 030
				0045	5	320 040
				0100	9	320 050
				0115	10	320 050

Date night of	Times UT	Notes	Station position (to nearest 0.5 degree)	Time UT	Max elev.	Limiting azimuths
					degrees	
25/26 (contd)				0130	12	320–030
				0145	11	330–030
			53.5° N 01° W	2315	10	000
				2350		350–010
				0040	15	335–045
				0120		315–060
				0150	15	315–070
				0210	Fade	030–060
				0225	No NLC	
			52° N 00.5° W	0045	5	000–050
				0145	NLC above fog	
26/27	2100–2140	Billows in broken trop. cloud, Sjælland and Bornholm. Patch of billows at Edmonton. No NLC (F).	56° N 12.5° E	2100–2125	30	045
			55° N 14.5° E	2140	22	000–022
28/29	0110–0210	Very faint parallel bands at Morpeth, seen only with binoculars.	55° N 01.5° W	0110	4	020–035
				0125		356–045
				0140	5	350–070
				0155	6	000–070
				0210	No NLC	
29/30		No NLC (F)				
30 June/1 July	2258–2311	Bands and billows in trop. cloud gaps, Edinburgh. No NLC (F).	56° N 03° W	2258	12	–030
				2311	32	335–020
3/4	2200–2230	Faint veil in trop. cloud gaps, Jämsä. No NLC anywhere else in Finland, or Alberta.	62° N 25° E	2200–2230	20	355–010
5/6	1920–0246	Extensive display, bands, billows, whirls; Finland, Britain, Denmark. No NLC in Alberta.	63° N 27.5° E	2130	24	015–050
				2150	NLC visible	
				2230	24	005–042
			62.5° N 27.5° E	2120	No NLC	
				2150	NLC suspect	
				2215	16	000–040
				2235	30	005–045
				2300–2315	36	000–290
			62° N 25° E	2200–2245	40	035–050
			60.5° N 25° E	2215	No NLC	
				2300	20	280–000
				2315	22	280–010
				2330–2345	22	280–350
			60.5° N 22° E	2230	15	300–330
				2245	20	245–050
				2300	22	245–055
				2315	22	245–035
				2330	25	250–090
				2345	15	250–090
			56° N 12.5° E	1920–2215	Bands	000
			56° N 09° E	2315	12	338–042
				2355	20	326–060
				0035	25	316–062
				0100	46	296–038
				0115	27	298–048
				0130	18	274–022
				0140	11	272–006
				0145	Faint NLC	
			56° N 03° W	0040–0200	30	330–060
			56° N 04.5° W	2252–2330	45	330–015
			55.5° N 04.5° W	0125–0131	25	000
			54° N 01° W	0045–0115	NLC present	
			52° N 01° W	0040	3	
				0246	16	
6/7	2230–2240	Faint bands at Rønne, NLC observed at Fort McMurray, Alberta. No NLC (F, G).	55° N 14.5° E	2230–2240	13	315–022
7/8	2144–2155	Very faint bands and billows at Itegem. No NLC (D, F).	51° N 04.5° E	2144	10	343–006
				2155	NLC with binocs.	
8/9		No NLC (B, F)				
9/10	2300–2345	Very faint NLC patches among cirrus suspected at Edinburgh. No NLC (B, F).	56° N 03° W	2300	45	330–030
				2315	50	300–055

Date night of	Times UT	Notes	Station position (to nearest 0.5 degree)	Time UT	Max elev. *degrees*	Limiting azimuths
9/10 (contd)				2330	55	330–055
				2345	NLC suspect	
10/11	2045–0000	Brilliant and extensive display throughout Finland except far north. All forms visible well into southern sky. SSE movement.	65.5° N 24.5° E	2200–2230	No NLC	
			65° N 25.5° E	2200–2230	No NLC	
			63° N 23° E	2130–2230	No NLC	
			62.5° N 27° E	2200	166	240–120
				2215	166	240–120
				2230	160	250–140
				2245	NLC present	
			62° N 25° E	2145–2245	35	350–045
			61° N 29° E	2145	150	190–100
				2215	150	210–120
				2245	150	210–090
				2300	150	210–090
			61° N 21.5° E	2045–2115	No NLC	
			60.5° N 27° E	2100–2130	50	160–080
			60.5° N 22.5° E	2100	No NLC	
				2120	Bands	270
				2145	145	220–120
				2200	145	230–080
				2215	140	260–080
				2230	125	220–080
				2245	130	250–135
				2300	145	260–100
				2315	160	250–140
				2330	140	260–110
				2345	155	255–140
				0000	140	235–100
			60° N 25° E	2050–2310	NLC extensive	
11/12	2020–2330	Bands in SW Finland but negative reports from rest of country.	61° N 23.5° E	2020–2100	22	210–270
			60.5° N 23.5° E	2145	22	011–055
				2200	40	320–050
			60° N 25° E	2200–2330	NLC suspect	
12/13		No NLC (F, G)				
13/14		No NLC (B, D)				
14/15	2040–2340	Minor display, bands and billows, Finland. SW movement.	62.5° N 27° E	2215	NLC present	
				2230	162	250–105
				2245–2315	160	235–170
			62° N 25° E	2150	60	340–045
				2210	65	330–045
			61° N 21.5° E	2200–2230	No NLC	
			60° N 25° E	2040–2340	45	
15/16	2025–2225	Minor display, bands and billows, Copenhagen and Alrö. No NLC (B).	56° N 10° E	2125	30	270–045
			55.5° N 12.5° E	2205–2225	7	000
16/17	2030–2330	Extensive, moderate to bright display over Finland. All forms, SW movement.	63° N 27.5° E	2200	36	250–090
				2230	40	170–230
				2305–2330	70	190–100
			63° N 23° E	2100–2130	25	240–260
			62.5° N 27° E	2045	NLC present	
				2145	160	210–120
				2200	160	190–150
				2230	35	265–090
				2245	90	240–120
			62° N 25° E	2150	70	240–060
				2220	50	250–065
				2240	40	270–050
				2310	60	250–045
			61° N 29° E	2115	60	170–010
				2130	80	185–020
				2145	90	000–190
						275–340
				2200	90	130–100
			61° N 23° E	2020–2140	No NLC	
			60.5° N 22.5° E	2030	No NLC	
				2100	NLC present	
				2130	90	220–060

Date night of	Times UT	Notes	Station position (to nearest 0.5 degree)	Time UT	Max elev.	Limiting azimuths
					degrees	
16–17 (contd)				2145	85	250–065
				2200	70	260–080
				2215	45	285–030
			60° N 25° E (Helsinki)	2100–2130	45	290–045
			60° N 25° E (Kaivopuisto)	2121–2300	45	250–335
17–18	0125–0240	Faint bands and billows in trop. cloud, Morpeth. No NLC (B, D).	55° N 01.5° W	0125	8	Cloud–038
				0140	9	340–035
				0155	12	336–035
				0210	15	–040
				0225	14	330–036
				0240	14	335–020
18–19	2030–2339	Moderate display, all forms, Finland.	65.5° N 24.5° E	2145–2230	No NLC	
			63° N 27.5° E	2205	24	290–340
				2215	26	280–340
				2230	35	250–340
				2250	24	260–330
			63° N 23° E	2115–2230	15	350–000
			62.5° N 27° E	2200	32	265–340
				2215–2300	NLC present	
			62° N 25° E	2130–2300	30	280–010
			61° N 29° E	2030–2130	No NLC	
			60.5° N 22.5° E	2100	No NLC	
				2130	15	340–020
				2230	15	330–030
			60° N 25° E	2100–2130	No NLC	
				2140	NLC	330
				2200	8	320–000
				2215	13	305–015
				2230	15	295–015
				2245	17	300–005
				2307	22	283–010
				2331	28	280–000
19–20	2015–2210	Veil suspected at Ilo (Finland). Other Finnish stations negative. No NLC (B, D, G).				
20–21	2000–2345	Bands reported at Helsinki, other Finnish stations negative. No NLC (D, G).	60° N 25° E (Helsinki)	2130–2250	No NLC	
				2300	30	330–015
				2321	NLC faint	
			60° N 25° E (Kaivopuisto)	2300–2330	NLC present	
			60° N 25° E (Konala)	2115–2140	50	270–000
21–22	0005–0100	Faint bands Vildbjerg, also Edmonton.	56° N 09° E	0005	6	342–020
				0030	8	342–022
				0100	Trace	000–010
22–23	2000–0015	Bright and extensive display over Finland, all forms. Possible SW drift. No NLC (G).	65.5° N 24.5° E	2200–2232	25	270–325
			65° N 25.5° E	2200	No NLC	
				2210	60	310–060
				2245	No NLC	
			63° N 27.5° E	2140	16	340–050
				2200	20	310–020
				2225	24	280–010
			62.5° N 27.5° E	2115	16	010–040
				2200	18	290–030
				2215	30	280–025
				2245	30	306–330
			62.5° N 27° E	2115	15	315–000
				2145	20	300–020
				2215	30	321–015
				2245	8	300–045
				2300	12	290–040
				2315	8	290–040
				2330	10	285–040
				2345	8	345–020
				0000	NLC present	
			62.5° N 25.5° E	2120–2235	25	

Date night of	Times UT	Notes	Station position (to nearest 0.5 degree)	Time UT	Max elev.	Limiting azimuths
					degrees	
22/23 (contd)			62° N 25° E	2200	30	320–025
				2220	25	315–010
				2235	20	310–000
				2330	15	315–350
			61° N 23° E	2020–2050	No NLC	
			60.5° N 22.5° E	2125	NLC present	
				2145	9	330–040
				2200	10	325–035
				2215	10	325–025
				2230	12	325–025
				2245	13	320–020
				2300	13	320–025
				2315	8	310–020
			60° N 25° E	2045	NLC low	
				2119	NLC present	
				2127	7	348–005
				2150	8	346–005
				2200	10	335–010
				2224	10	331–005
				2237	10	322–005
				2300	5	320–330
				2322	2	352
				2330	7	315–000
				0012	NLC present	
23/24		No NLC (F)				
24/25		No NLC (D, F)				
25/26	2040–0150	Very bright and extensive display, all forms, Finland and Denmark	65.5° N 24.5° E	2200–2245	No NLC	
			65° N 25.5° E	2200	145	005–120
				2240	155	280–005
				2305	30	020–090
				2320	25	015–070
			63° N 27.5° E	2100–2115	40	330–045
			63° N 23° E	2115–2245	30	000–090
						270–300
			62.5° N 27° E	2045	NLC present	
				2145	110	300–120
				2215	95	270–120
				2230	NLC in cloud	
			62° N 25° E	2100	30	300–045
				2120	40	280–050
				2140	35	270–055
				2200	30	270–045
				2230	30	300–040
			61.5° N 23.5° E	2102	20	300–048
				2130	20	300–055
				2145	20	312–055
				2205	22	336–048
				2225	22	336–060
				2245	20	310–060
			61° N 23° E	2040–2150	60	240–350
			60.5° N 22° E	2110	NLC	NE and NW
				2130	15	280–050
				2145	15	280–055
				2200	15	280–045
				2230	17	285–060
				2300	18	300–090
				2330	35	280–095
				0000	60	280–115
			60° N 25° E	2115	15	N
				2255	6	002–010
				2320	23	327–060
				2340	57	290–080
				2355	61	280–095
				0000	61	
			60° N 24.5° E	2100	8	320–050
				2130	12	290–035
			56° N 10° E	2055–0110	15	315–090
			56° N 09° E	2115	10	334–040
				2145	11	330–038
				2215	11	342–028

Date night of	Times UT	Notes	Station position (to nearest 0.5 degree)	Time UT	Max elev.	Limiting azimuths
					degrees	
25/26 (contd)				2245	6	340–040
				2315	6	340–030
				2345	7	332–032
				0015	12	338–046
				0045	13	338–048
				0100	12	340–064
				0130	10	356–035
				0150	10	002
26/27		No NLC (F)				
27/28	2045–2345	Small patch of bands very low at Edinburgh. Fairly small display of bands and billows, Finland.	63° N 27.5° E	2130	65	000–030
			62° N 25° E	2045–2110	No NLC	
			60° N 25° E	2121	10	WNW
				2312	NLC	N
				2328	8	337–340
				2334	8	330–005
				2342	8	325–000
			56° N 03° W	2243	3	035–040
				2300	3	010–040
				2315	3	356–040
				2345	3	Cloud
28/29	2040–2300	Faint to moderate bands over USSR, seen from Finland. All forms at Rautalampi.	63° N 27.5° E	2100	15	045–070
				2125	17	060–080
				2145–2200	8	350–050
			62.5° N 27° E	2215	14	000–070
				2245	NLC present	
			61.5° N 23.5° E	2040–2130	No NLC	
			61° N 29° E	2100	10	010–050
				2115	12	030–040
				2145	No NLC	
			60.5° N 22.5° E	2045–2125	No NLC	
29/30 to 30/31		No NLC (F)				
1/2 Aug	2115–2345	Bands visible in trop. cloud gaps, E Finland.	63° N 27.5° E	2115–2130	34	340–000
			62.5° N 27° E	2330–2345	10	010–050
2/3	2015–2230	Moderate to bright display, all forms, Finland. SW drift.	63° N 23° E	2030–2230	No NLC	
			62.5° N 27° E	2030–2105	No NLC	
				2115	18	340–030
				2130	20	320–030
				2145	20	330–030
				2200	20	320–040
				2230	26	305–040
			61.5° N 23.5° E	2040	No NLC	
				2120	9	330–030
				2135	11	312–024
			61° N 29° E	2045	10	000–020
				2130	10	320–025
				2200	10	320–025
			61° N 21.5° E	2015–2100	No NLC	
3/4		No NLC (B, F)				
4/5	2030–0000	Faint bands in trop. cloud gaps, Rautalampi.	62.5° N 27° E	2300–2315	12	020–030
				2345–0000	15	350–015
			62° N 25° E	2030–2200	No NLC?	
			61° N 21.5° E	2030–2130	No NLC	
5/6		No NLC (F)				
9/10	1900–2330	Slight bands at Maksamaa and Lapua, W Finland.	65.5° N 24.5° E	2230–2330	No NLC	
			63.5° N 22° E	2220–2245	15	315–000
			63° N 23° E	2200–2230	10	340–000
			60.5° N 27° E	1900–2100	No NLC	
10/11 to 11/12		No NLC (F)				
12/13	2215–2340	Small moderately bright NLC, bands and billows, E Finland. Patches of billow suspected at Detmold despite moon.	65.5° N 24.5° E	2245–2340	15	000–030
			63° N 28.5° E	2300–2330	10	000–040

Date night of	Times UT	Notes	Station position (to nearest 0.5 degree)	Time UT	Max elev. *degrees*	Limiting azimuths
12/13 (contd)			63° N 27.5° E	2215–2245	12	010–030
			52° N 09° E	2300	NLC?	
13/14	1930–0234	Faint bands and whirls at Rautalampi. Short-lived and faint NLC at Viby (Funen).	65.5° N 24.5° E	2115–0045	No NLC	
			63° N 23° E	2000–2245	No NLC	
			62.5° N 27° E	2010	NLC present	
				2015	150?	210–090
				2030	NLC present	
			62.5° N 24.5° E	1940–2030	45	270–000
			62° N 25° E	2000–2130	45	310–030
			61.5° N 23.5° E	2050	9	300–012
				2100	9	324–000
			60.5° N 22.5° E	1930–0100	No NLC	
			55.5° N 10.5° E	0232	NLC trace	N
14/15	1945–0100	Small veil suspected at Tampere. 4 other Finnish stations negative.	61.5° N 23.5° E	2115–2125	5	300–000
15/16		No NLC (F)				
16/17	2000–2300	Faint bands and billows at Kemi. 2 other Finnish stations negative.	65.5° N 24.5° E	2230–2300	10	335–010
17/18 to 20/21		No NLC (F)				
23/24	1900–2100	Small brightish bands at Lapua.	63° N 23° E	2000–2100	30	
			62° N 25° E	1900–2000	No NLC	
24/25		No NLC (F)				
26/27 to 28/29		No NLC (F)				
29/30	1830–2230	Faint veil at Ilo? No NLC at Helsinki and Kemi.	61° N 23° E	1830–1910	20	330–000
30/31	1900–2230	Brightish veil suspected at Pertteli, no NLC at 3 other Finnish stations.	60.5° N 23.5° E	1900	32	280–045
				1910	45	270–049

Photographs

13/14 June	2238	Rønne	J.Ø. Olesen
14/15	0005–0021	Edinburgh (Blackford)	N. Bone
	0015–0045	Edinburgh (Joppa)	D. Gavine
	2317–0145	Morpeth	A. McBeath
	2249, 2338	Vildbjerg	H. Andersen
15/16	0015–0045	Milngavie	A. Simmons
	0100–0136	Stirling	A. Smeaton
	0130–0147	Edinburgh	D. Gavine
	0130–0245	Morpeth	A. McBeath
23/24	2235	Wakefield	M.D. Taylor
	2240	Heswall, Wirral	P. Irons
5/6 July	2315	Milngavie	A. Simmons
	0040, 0100	Vildbjerg	H. Andersen
15/16	2210	Rønne	J.Ø. Olesen
17/18	0125–0255	Morpeth	A. McBeath
18/19	2307	Helsinki	D. Frydman
22/23	2207–2249	Helsinki	D. Frydman
25/26	2311–2336	Helsinki	D. Frydman
	2215–0015	Vildbjerg	H. Andersen
	0040	Rønne	J.Ø. Olesen
27/28	2254–2303	Edinburgh (Blackford)	N. Bone
	2300–2315	Edinburgh (Joppa)	D. Gavine

551.509.324.1

Convective cloud forecasts from the Meteorological Office fine-mesh model

By T. Davies

(Meteorological Office, Bracknell)

Since March 1986, charts showing convective cloud tops and depths, as produced by the fine-mesh 15-level numerical model, have been available in the Central Forecasting Office (CFO) of the Meteorological Office. Two sets of charts are produced for the analysis time (T) and for each 6 hours of the forecast from T+18 to T+36, and cover the area of the fine-mesh model (30–80° N, 80° W–40° E). The charts are specifically tailored to the needs of the aviation forecasters in the International Civil Aviation Organization Regional Area Forecast Centre located within CFO.

One set of charts indicates where convective cloud tops are above 20 000 ft and depths are in excess of 10 000 ft. These are used to determine those regions where cumulonimbus clouds are thought likely to penetrate to significant flight levels (25 000 ft and above). Examples of the part of these charts covering the British Isles are shown in Figs 1 and 2 for cloud tops and depths respectively. The second set of charts shows the position of clouds with tops between 10 000 and 20 000 ft, and depths in excess of 5000 ft, and these are of particular use for lower-level flights.

The two sets of charts can be used to build a picture of the model's convective cloud. This can help to assess the convective component of rainfall in some situations since, for output purposes, dynamic (i.e. large-scale) rainfall symbols are printed in preference to convective symbols when both types of rainfall occur. Fig. 3 shows the conventional model output of surface pressure and rainfall valid at the same time as the cloud tops and cloud depths given in Figs 1 and 2. Notice that only dynamic rainfall symbols appear over England whereas the convection charts show that there is a convective element to the rain.

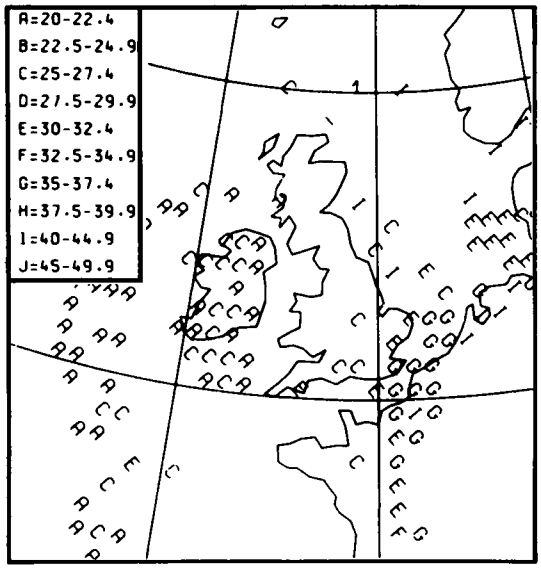

Figure 1. Fine-mesh 15-level numerical model T+18-hour forecast of convective cloud tops (key gives heights in thousands of feet), based upon data time 00 GMT, 3 August 1986.

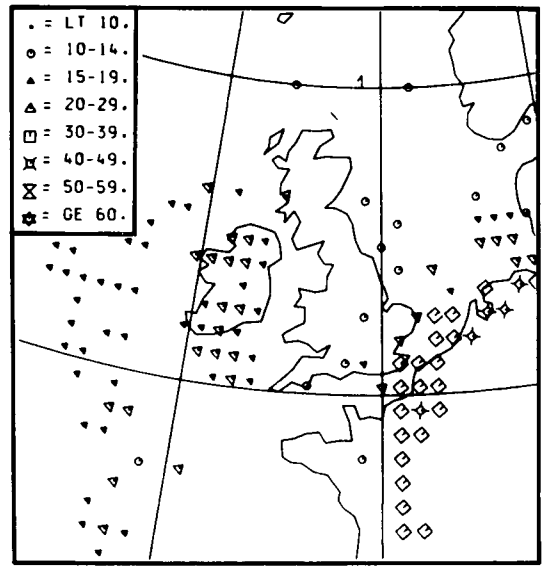

Figure 2. As Fig. 1 but for convective cloud depths (key gives depths in thousands of feet).

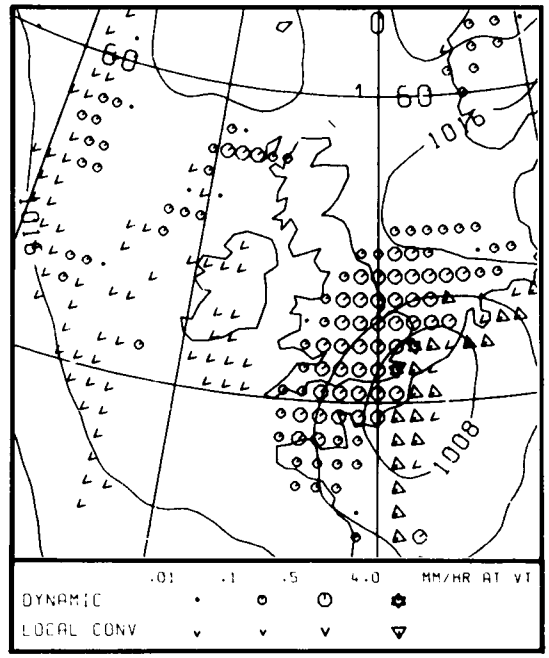

Figure 3. As Fig. 1 but for surface pressure (mb) and rainfall (see key).

The information displayed in the convection charts is obtained from the model's deep convection scheme which is based on parcel theory modified by entrainment. The cloud base is defined as the bottom of the first model layer for which moist convection takes place. A buoyant parcel is assumed to rise through the unstable atmosphere, gradually losing mass by detrainment, until it is no longer buoyant — this level is taken to be the cloud top. In the model it is possible for convection to restart after terminating at a lower level, but the cloud charts identify only the lowest convective layers at a particular grid point.

The charts have been well received by the forecasters who find them very useful in preparing significant weather charts and for issue of SIGMETs (warnings of severe weather to aircraft in flight).

Acknowledgement

The convective cloud chart output for CFO was developed by Mrs A.J.K. Small.

Notes and news

EUMETSAT

On 18 June 1986 a special inter-governmental meeting was convened in Paris to consider the status of EUMETSAT (EUropean METeorological SATellite organization). Sixteen European states agreed that the organization should be authorized to begin its work immediately. A few days later the first meeting of the EUMETSAT Council appointed John Morgan, then Assistant Director (Satellite Meteorology) in the Meteorological Office, as its first Director; it was also decided that the headquarters should be located in Darmstadt, Federal Republic of Germany.

EUMETSAT has been created to establish, maintain and exploit European systems of operational meteorological satellites. Its first task will be to carry overall responsibility for the Meteosat Operational Programme, though this programme will be operated by the European Space Agency on behalf of EUMETSAT. Furthermore it will evaluate existing and future programmes, and will contribute to the development of space meteorology techniques and meteorological observing systems that use satellites.

The Professor Dr Vilho Vaisala Award

The World Meteorological Organization (WMO) has agreed to a trust fund being set up to finance an annual award entitled the 'Professor Dr Vilho Vaisala Award' which is named after the well known meteorologist and instrument maker. The purpose of the award is to encourage and stimulate interest in research concerned with instruments and methods of observations which support WMO programmes. It is awarded for the best published paper on these topics during the previous 18 months.

The Executive Council of WMO selected Chris Collier, until recently Assistant Director (Operational Instrumentation) in the Meteorological Office, to be the first recipient of the award. It was given in recognition of his paper on the 'Accuracy of rainfall estimates by radar' published in the *Journal of Hydrology* in 1986. In Part I of the paper the provision of radar data for both rainfall and flood forecasting is discussed. In particular the accuracy of the gauge-calibrated radar estimates of rainfall, when compared with data from rain-gauges, is considered over river sub-basins of up to 200 km^2. An analysis is described in Part II of the way in which radar data, together with data from telemetering rain-gauges, should be used for flood forecasting. In Part III a simple hydrological model is used to assess the effects of errors in estimates of rainfall made by radar on predictions of river flow.

The award was presented to Mr Collier on the 50th Anniversary of Vaisala OY in Helsinki, Finland on 5 September 1986.

Reviews

Air: composition and chemistry, by P. Brimblecombe. 170 mm × 240 mm, pp. viii + 224, *illus.* Cambridge University Press, 1986. Price £25.00 (hardback) £8.95 (paperback).

In recent years a number of textbooks on atmospheric chemistry have been published and perhaps the natural question to ask is whether we really need another one. This book is aimed at the level of the young scientist or perhaps interested meteorologist compared with the more learned works by G. Brasseur and S. Solomon (*Aeronomy of the middle atmosphere*, Dordrecht, D. Reidel Publishing Company, 1984), R.P. Wayne (*Chemistry of atmospheres*, Oxford University Press, 1985), and that edited by J.S. Levine (*The photochemistry of atmospheres. Earth, the other planets and comets*, London, Academic Press, 1985).

The book is divided into nine chapters which give a broad brush treatment of virtually the whole subject area from gas phase chemistry to the atmospheres of the planets. In general, I felt that the more simple the concept, the more irksome the description became. For example, on page one the reasons for supposing the air to be a mixture of gases as opposed to a single compound are somewhat laboured and the statement that, 'if it were a compound the formula would be $N_{15}O_4$ and this seems rather unlikely' does not seem to be very scientific. Later in the same chapter the concept of average residence time for species is not as clear as it could be with the word 'average' not properly defined. More worrying, though, was the statement that, '... where the environment cools less rapidly with height than the adiabatic lapse rate an inversion is said to have formed' (page 118).

The author has taken the step of giving just a few references on the subject matter of each chapter and I think in general this has worked well. However, there are two major omissions — the book by Brasseur and Solomon from the references of Chapter 8, and the book by Levine from the references of many chapters but especially of Chapter 9. In fact Chapter 8 is quite inadequate in scope when one considers the biological effects of potential damage to the ozone layer due to anthropogenic activities, and the whole concept of interaction between chemistry and dynamics in the middle atmosphere is not raised at all. In Chapter 9 omission of references to the book by Levine, which describes the chemistry of the other planets in much more depth, is equally serious. Levine's book, though, quotes methane concentrations on Jupiter and Saturn some 2½ and 5½ times greater. This is confusing bearing in mind that both sets of figures are presumably based on the same Voyager data. There are also small differences in some other constituents.

I think the book could also have been improved by the addition of two more chapters — one on the theoretical techniques of chemical modelling and another on the techniques of measuring minor constituents. As regards chemical modelling the nearest that the author gets to it is in discussing reaction rates in Chapter 3 on gas phase chemistry; and in discussing the reaction $2NO + O_2 \rightarrow 2NO_2$ a factor of 2 finds itself on the wrong side of several equations. Despite reading every word of the book (I from insomnia!) suffer I could find few references to measuring techniques.

The best parts of the book are Chapters 6 and 7 dealing with the sources and effects of air pollution which, on the basis of their length (together they cover over one third of the book), are the author's main areas of expertise. Here some very interesting facts on the effects of pollution on human health may be found. For example, cigarette smoke contains about 400 parts per million by volume of carbon monoxide which lies in the category whose health effects include headaches and nausea. As a cautionary note, although the pollution chemistry of the troposphere is described in much more detail than topics in other chapters, I wonder whether some clarity in the scientific concepts has been lost. For example, a paradox such as why does nitric oxide destroy ozone in the stratosphere but produce ozone in the troposphere is not brought out in the text whereas I think a book at this level should raise such questions.

Despite these criticisms the book is quite appropriate, in general, to the audience to which it is addressed (students taking courses in environmental sciences, ecology and chemistry) but would probably not appeal very much to active researchers in the field. So the answer to the question raised in my first paragraph, i.e. do we really need another textbook, is, I think, a qualified 'yes'.

J. Austin

World survey of climatology, Volume 1A: General climatology, 1A, by A.Kessler. 217 mm × 300 mm, pp. xii + 224, *illus*. Elsevier Science Publishers, Amsterdam, London, New York, Tokyo, 1985. Price US $55.50, Dfl 150.00.

This fine book is divided into several sections; firstly a historical résumé of climatology (the earliest reference is 'Halley 1687'), then a chapter on the earth–atmosphere heat and radiation budget, which was unfortunately unread as pages 5 to 20 inclusive were missing in the reviewer's copy. The book is historical in another aspect, since printing was delayed by a change of editor and 'slow' contributors, hence one may get some feel for the growth of the science during the last 15 years.

Subsequent chapters on the net radiation, latent heat flux and sensible heat flux (all at the earth's surface) are thoroughly explored including their diurnal and annual variability, on a global scale, with consideration being given to types of surface and the vegetation thereon. Many tables and diagrams are used to support the text, all neatly displayed, but some of the captions are, of necessity I suppose, rather cumbersome. I especially liked Figure 15 which is a fold-out (usually frowned upon) of the net radiation

at selected sites around the world, displayed by month and hour of day with a helpful inset showing the location of the places and their relative positions. This helps comparison, but the author's discussion occurs ten pages later.

Finally, there is a chapter on heat flux into the surface, with all the complications of ablation, biomass and oceanic transport investigated. For oceanic heat flux, the author states (with surprise) that the sign changes three times at Ship 'V' between 1956 and 1970; in fact I made it even more surprising at six times — perhaps a case of different interpretation. It is hereabouts that a few tentative remarks are made about climatic changes and the oceans' importance to them. In this chapter there is also an interesting discussion about the variable ground-water temperature associated with urbanization (Cologne is used as the example) and a statement about the water temperature at 28 metres beneath the Paris Observatory having risen by nearly 2 °C during this century up to 1969.

There are comprehensive reference sections and appendices, with Appendix III being a conversion table to 'modern' SI units, since the energy unit used in the book, which is one of a large series, is calories and is to be used throughout the series for consistency. The subject index is disappointing after the earlier thoroughness, mainly seeming to concern itself with various types of earth cover.

With over 70 figures and over 70 tables scattered throughout the book, it might have been better to have arabic numerals for tables as well as for figures, and/or keep a section at the end of the book for tables. Many times one is confused, for example on page 182 one is referred to Tables LVIII and XLIII and Figure 46 simultaneously, when Figure 73 is on the current page and Table LXX is on the previous page, which becomes rather frustrating and wearing on the pages.

Nevertheless, the book has been compiled with great care, accuracy and enthusiasm in good readable English and, despite the weighty subject, it is entertaining, albeit possibly unconsciously as in the sentence, 'The climate of the small isolated island is extremely maritime'. What else?

I am reviewing the book as a non-expert, but would recommend it, to anyone interested in meteorology, for browsing or reference.

S.H. Barker

Books received

The listing of books under this heading does not preclude a review in the Meteorological Magazine at a later date.

Physics and chemistry in space, Vol. 13: Photochemistry of the atmospheres of Mars and Venus, by V.A. Krasnopolsky (Berlin, Heidelberg, New York, Tokyo, Springer-Verlag, 1986. DM 240.00) gives a detailed description of the chemical structure of the atmospheres of Mars and Venus, and the chemical and physical processes that define the properties of these atmospheres. It compiles experimental and theoretical data collected over the last decade in ground-based observations and, by Soviet and American flyby systems, orbiters and descent probes. The author reviews various methods for determining the chemical composition of planetary atmospheres, discusses the reliability of the experimental results critically, and compares these results with predictions based on photochemical modelling.

Notes on numerical fluid mechanics, Vol. 13: Proceedings of the Sixth GAMM-Conference on numerical methods in fluid mechanics, edited by D. Rues and W. Kordulla (Wiesbaden, Friedr. Vieweg and Sohn, 1986. £31.00) contains the 51 papers presented at this conference which was held at Göttingen in the Federal Republic of Germany on 25–27 September 1985. The papers cover a broad range of topics from the mathematical development and investigation of algorithms to applications to fluid mechanical problem in acoustics, aerodynamics, car aerodynamics, gas dynamics, hydrodynamics, meteorology, oceanography, turbomachinery, etc. A report on the GAMM-Workshop 'The efficient use of vector computers with emphasis on computational fluid dynamics' is included.

Satellite photograph — 24 August 1986 at 1552 GMT

The satellite picture is a NOAA-9 visible image over the mid-Atlantic (British Isles extreme right). Two vortices are defined by low-level clouds -- a shallow low near the tip of southern Greenland, and a less well-defined swirl showing the remains of ex-hurricane Charley (centre bottom).

A vast 'head' of cloud is present well in advance of Charley, composed of mostly thick middle- and upper-level cloud, although the forward portion is largely transparent cirriform cloud. Similar cloud heads are often observed prior to rapid cyclogenesis.

Subsequent satellite images suggest that the cloud swirl associated with the hurricane weakened, whilst the intense circulation that brought severe gales and considerable rainfall over England, Wales and the Republic of Ireland on 25 August was probably associated with a new low that formed several hundred kilometres to the north-east.

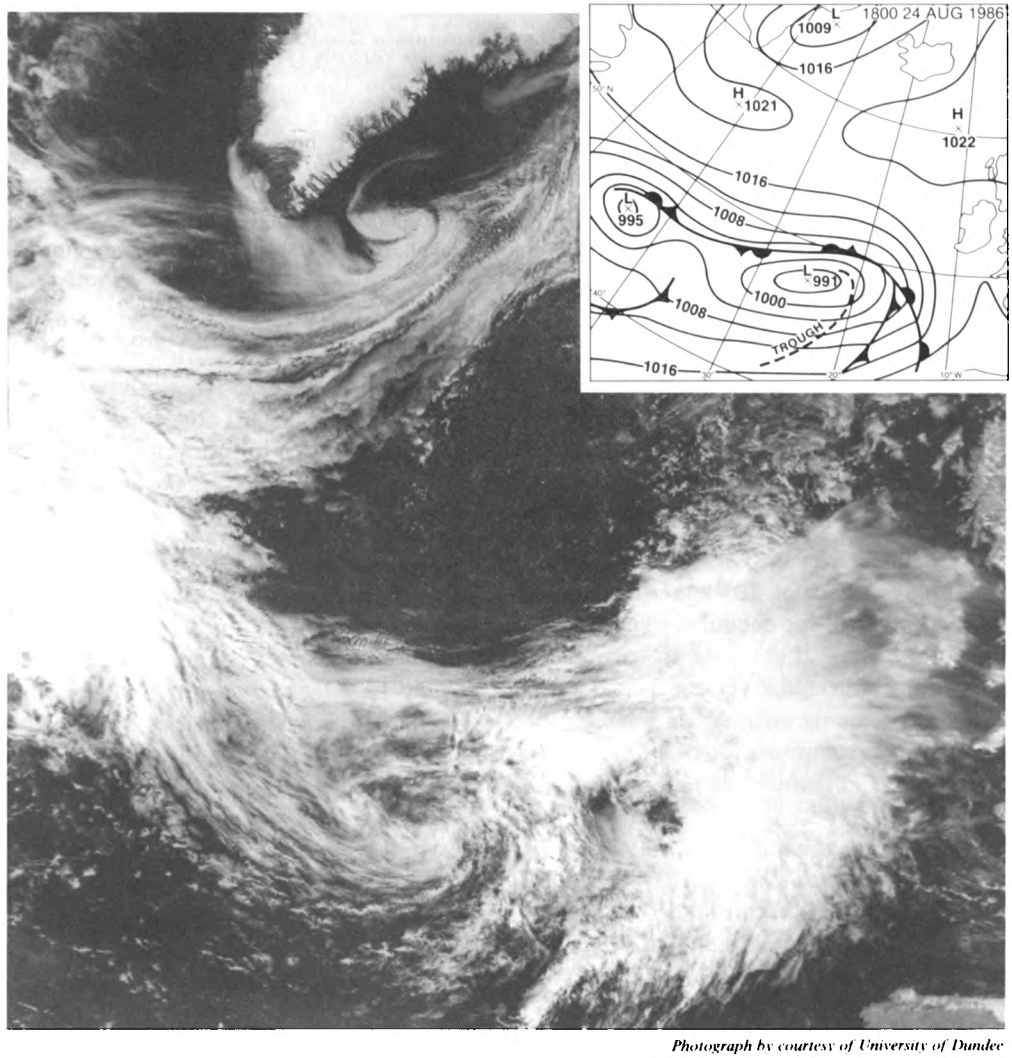

Photograph by courtesy of University of Dundee

Meteorological Magazine

GUIDE TO AUTHORS

Content

Articles on all aspects of meteorology are welcomed, particularly those which describe the results of research in applied meteorology or the development of practical forecasting techniques.

Preparation and submission of articles

Articles for publication and all other communications for the Editor should be addressed to the Director-General, Meteorological Office, London Road, Bracknell, Berkshire RG12 2SZ and marked 'For *Meteorological Magazine*'.

Articles, which must be in English, should be typed, double-spaced with wide margins, on one side only of A4-size paper. Tables, references and figure captions should be typed separately.

Spelling should conform to the preferred spelling in the *Concise Oxford Dictionary*.

References should be made using the Harvard system (author, date) and full details should be given at the end of the text. If a document referred to is unpublished, details must be given of the library where it may be seen. Documents which are not available to enquirers must not be referred to.

Tables should be numbered using roman numerals and provided with headings. We consider vertical and horizontal rules to be unnecessary in a well-designed table; spaces should be used instead.

Mathematical notation should be written with extreme care. Particular care should be taken to differentiate between Greek letters and Roman letters for which they could be mistaken. Double subscripts and superscripts should be avoided, as they are difficult to typeset and difficult to read. Keep notation as simple as possible; this makes typesetting quicker and therefore cheaper, and reduces the possibility of error. Further guidance is given in BS1991: Part 1: 1976 and *Quantities, Units and Symbols* published by the Royal Society.

Illustrations

Diagrams must be supplied either drawn to professional standards or drawn clearly, preferably in ink. They should be about 1½ to 3 times the final printed size and should not contain any unnecessary or irrelevant details. Any symbols and lettering must be large enough to remain legible after reduction. Explanatory text should not appear on the diagram itself but in the caption. Captions should be typed on a separate sheet of paper and should, as far as possible, explain the meanings of the diagrams without the reader having to refer to the text.

Sharp monochrome photographs on glossy paper are preferred: colour prints are acceptable but the use of colour within the magazine is at the Editor's discretion. In either case contrast should be sufficient to ensure satisfactory reproduction.

Units

SI units, or units approved by WMO, should be used.

Copyright

Authors wishing to retain copyright for themselves or for their sponsors should inform the Editor when they submit contributions which will otherwise become UK Crown copyright by right of first publication.

It is the responsibility of authors to obtain clearance for any copyright material they wish to use before submitting it for publication.

Free copies

Three free copies of the magazine are provided for authors of articles published in it. Separate offprints for each article are not provided.

Meteorological Magazine

November 1986

Vol. 115
No. 1372

CONTENTS

Page

Experimental monthly long-range forecasts for the United Kingdom. Part II. A real-time long-range forecast by an ensemble of numerical integrations.
J.M. Murphy and T.N. Palmer ... 337

The Spanish plume — testing the forecaster's nerve. R.M. Morris ... 349

Ocean and atmosphere interact! S.J. Foreman ... 358

Noctilucent clouds over western Europe during 1985. D.M. Gavine ... 360

Convective cloud forecasts from the Meteorological Office fine-mesh model.
T. Davies ... 361

Notes and news
EUMETSAT ... 372
The Professor Dr Vilho Vaisala Award ... 373

Reviews
Air: composition and chemistry. P. Brimblecombe. *J. Austin* ... 373
World survey of climatology, Volume 1A: General climatology, 1A. A. Kessler. *S.H. Barker* ... 374

Books received ... 375

Satellite photograph — 24 August 1986 at 1552 GMT ... 376

Contributions: it is requested that all communications to the Editor and books for review be addressed to the Director-General, Meteorological Office, London Road, Bracknell, Berkshire RG12 2SZ, and marked 'For *Meteorological Magazine*'. Contributors are asked to comply with the guidelines given in the *Guide to authors* which appears on the inside back cover. The responsibility for facts and opinions expressed in the signed articles and letters published in *Meteorological Magazine* rests with their respective authors. Authors wishing to retain copyright for themselves or for their sponsors should inform the Editor when submitting contributions which will otherwise become UK Crown copyright by right of first publication.

Subscriptions: Annual subscription £27.00 including postage; individual copies £2.30 including postage. Applications for postal subscriptions should be made to HMSO, PO Box 276, London SW8 5DT; subscription enquiries 01–211 8667.

Back numbers: Full-size reprints of Vols 1–75 (1866–1940) are available from Johnson Reprint Co. Ltd, 24–28 Oval Road, London NW1 7DX. Complete volumes of *Meteorological Magazine* commencing with volume 54 are available on microfilm from University Microfilms International, 18 Bedford Row, London WC1R 4EJ. Information on microfiche issues is available from Kraus Microfiche, Rte 100, Milwood, NY 10546, USA.

ISBN 0 11 727839 4

ISSN 0026–1149

© Crown copyright 1986

Printed for HER MAJESTY'S STATIONERY OFFICE
by Delco Printing Co. Ltd. 10/86 Dd. 739131 C14.25